國立臺灣大學生命科學院生化科技學系

碩士論文

Department of Biochemical Science and Technology

College of Life Science

National Taiwan University

Master Thesis

以益生大腸桿菌衍生之奈米載體作爲 CRISPR-Cas12b 之遞送系統

Bactofection by Probiotic *E. coli* -Derived Nanocarriers for CRISPR-Cas12b Delivery

黃章衍

Chang-Yen Huang

指導教授：吳亘承 博士

Advisor: Hsuan-Chen Wu, Ph. D.

中華民國 112 年 7 月

July 2023

doi:10.6342/NTU202303502

國立臺灣大學碩士學位論文
口試委員會審定書
MASTER'S THESIS ACCEPTANCE CERTIFICATE
NATIONAL TAIWAN UNIVERSITY

以益生大腸桿菌衍生之奈米載體作為 CRISPR-Cas12b 之遞送系統

（論文中文題目）(Chinese title of Master's thesis)

Bactofection by Probiotic E. coli-Derived Nanocarriers for CRISPR-Cas12b Delivery

（論文英文題目）(English title of Master's thesis)

本論文係 黃章衍 (姓名) R10B22019 （學號）在國立臺灣大學生化科技學系完成之碩士學位論文，於民國 112 年 7 月 12 日承下列考試委員審查通過及口試及格，特此證明。

The undersigned, appointed by the Department of Biochemical Science and Technology on ___(date)_____ (month)_____ (year) have examined a Master's thesis entitled above presented by_____ (name)_____ (student ID) candidate and hereby certify that it is worthy of acceptance.

口試委員 Oral examination committee:

吳亘生

（指導教授 Advisor）

史有伶　　黃楓婷

系主任/所長 Director: 李昆達

Table of Content

doi:10.6342/NTU202303502

doi:10.6342/NTU202303502

doi:10.6342/NTU202303502

Table of Figures

doi:10.6342/NTU202303502

doi:10.6342/NTU202303502

doi:10.6342/NTU202303502

摘要

基因編輯系統 CRISPR-Cas (clustered regularly interspaced short palindromic repeats/CRISPR-associated proteins)自其發現以來，在醫療領域上具有重大應用與發展潛力，特別是在基因治療。然而 CRISPR-Cas 需要一個安全可靠、可廣泛、製造經濟化的運送系統，方以有效用於生物體的基因編輯與治療，目前的運送載體，例如病毒載體或人造聚合物往往面臨諸多挑戰，如安全因素或合成上的繁瑣複雜等。除此之外，CRISPR-Cas 本身的遞送形式也是一個考量重點，爲了避免外源基因插入宿主基因體的風險，使用信使核糖核酸 (mRNA) 或核糖蛋白 (ribonucleoprotein, RNP) 是較爲安全的形式。本研究意在建立一種新型的益生菌之 CRISPR-Cas RNP 遞送系統，以益生菌衍生之奈米載體作爲包裹和傳遞 RNP 的載體。具體來說，益生菌 *Escherichia coli* Nissle 1917 (EcN) 以基因敲落的方式，令其在分裂時產生不再分裂的微小細胞 (minicells)，同時讓 EcN 表達外源蛋白 Cas12b 使其在胞內組裝 Cas12b RNP。這些微小細胞會藉由表達外膜蛋白 invasin 以結合哺乳類細胞表面，並藉由表現 listeriolysin O 來釋放細菌表達的蛋白進入細胞內部，一旦微小細胞被吞入並在細胞的胞內體中裂解，Cas12b RNP 便可藉由核定位序列 (nucleus localization signal, NLS) 的幫助，運送到細胞核內完成基因編輯。同時在研究中，我們建構了 CRISPR 編輯報道細胞株 DGG.HeLa，以功能增益 (grain-of-function) 的方式來確認細胞是否有被成功編輯，在基因被成功編輯後，細胞才會生產綠色螢光蛋白 (green fluorescence protein; GFP) 。更具結果顯示，經由 minicells 運輸 Cas12b-sgRNA，我們能成功編輯 DGG.HeLa，並產生最高約 5% 之永久綠色系細胞株。在未來我們將繼續調整 minicells 系統，增加編輯效率與生醫應用性。

關鍵字：CRISPR-Cas 遞送、基因編輯、 *E. coli* Nissle 1917、微小細胞

doi:10.6342/NTU202303502

Abstract

CRISPR-Cas (clustered regularly interspaced short palindromic repeats/CRISPR-associated proteins) systems have an emerging utilization and research since its discovery, especially in gene therapy. A safe, universal, and affordable delivery platform is required when encountering *in vivo* editing. Current platforms such as viral vector and artificial polymer face several challenges, such as safety issues and complication in production. In addition, the form of delivered CRISPR-Cas is an issue to concern. It is commonly accepted that delivering RNP (ribonucleoprotein) and mRNA of CRIPSR-Cas are safer than delivering CRISPR-Cas DNA, to avoid possible gene integration. Here, we utilize a bioengineered probiotic-derived nanocarrier to deliver functional CRISPR-Cas12b RNP. Specifically, *Escherichia coli* Nissle 1917 (EcN) is engineered to produce non-proliferating minicells by gene knockout, as well as to express functional Cas12b RNP within the minicells. These minicells are capable of binding mammalian cells by expressing *Yersinia* outer membrane protein invasin, and are able to escape from endosome by expressing listeriolysin O. Once the minicells are engulfed and lysed within the targeting cell, Cas12b RNP would be transferred into nucleus by the assist of nuclear localization protein (NLS) to conduct further genome editing. In this study, we

doi:10.6342/NTU202303502

constructed a CRISPR-reporting cell line DGG.HeLa to specifically producing green fluorescence protein (GFP) only after CRISPR-editing via Cas12b-sgRNA minicells. As the result demonstrated in the research, the GFP-expressing stable DGG.HeLa cell line was created at the success rate of 5% via the engineered minicell system. We anticipate that further development of the CRISPR-minicell delivery system will increase the editing efficiency of future biomedical applications.

Keywords: CRISPR-Cas delivery, gene editing, *E. coli* Nissle 1917, minicell

doi:10.6342/NTU202303502

1. Introduction

Gene editing assisted therapy, or gene therapy, is a method for disease treatment by introducing exogenous genes or by modifying existing genes[1]. It has the potential to treat and eradicate a variety of illnesses, including hereditary diseases, cancer, AIDS, and allergies, which cannot be cured by conventional methods[2]. Numerous protocols have been developed in the laboratory, and many have further advanced from phase 2 (around 300 in total) to phase 4 (about 10 clinical trials)[3]. Among the current technical advancements of gene editing, the breakthrough of clustered regularly interspaced short palindromic repeats (CRISPR) has revolutionized the entire field of biotechnology and therapeutics, such as immunotherapy. In 2020, the Nobel Prize in Chemistry was awarded in recognition of the pioneering contributions of CRISPR[4]. On the basis of the ground-breaking CRISPR innovation, more strategic efforts are now being made to develop next-generation CRISPR technology with enhanced efficiency, safety, and cost-effectiveness. Detailed rationales and gene editing technologies are briefed in the following introductory sections.

doi:10.6342/NTU202303502

1.1 Gene Editing and CRISPR

In Nature, biology harnesses nucleases systems for genetic manipulation and processing for maintaining the biological integrity and survivability. Currently, a few forms of nucleases, acquired site-specificity and controllability, are chosen as ideal toolkits for biotechnological genetic editing[5]. For instance, zinc-finger nucleases (ZFNs) are the first artificial nucleases which is highly customizable and specific. ZFNs showed successful genome editing in model organisms and mammalian cells[5]. Transcription activator-like effectors nucleases (TALENs), originated from ZFNs, also have the ability to conduct site-specific genome editing. However, the design and manufacturing of ZFNs or TALENs, protein-based recognition effectors, is quite laborious and they also suffer from certain degree of inaccurate cleavage and off-target effects[6, 7].

CRISPR was first discovered in *Escherichia coli* and described in 1987[8], but it was until 2002 that the discovery of the role of CRISPR-associated 9 (Cas9) protein, crRNA and tracrRNA in 2007 and 2011 that made CRISPR-Cas a technically-feasible tool for gene editing[9]. In 2013, Cong et al. and Mali et al. used Cas9 to editing mammalian cells and showed great success in genome alteration[10, 11], in which the

doi:10.6342/NTU202303502

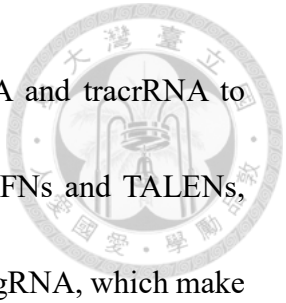

novel single guide RNA (sgRNA) was designed in place of crRNA and tracrRNA to induce specific editing in mammalian genome. In comparison to ZFNs and TALENs, CRISPR-Cas9 only requires the rapid and straightforward design of sgRNA, which make it a more versatile and universal strategy[7]. CRISPR was heavily investigated since the discovery of its programmable site-specific nuclease activity[7]. Many *in vitro* tests were done and demonstrated the potential of *in vivo* genome editing[12].

1.1.1 CRISPR-Cas9 and CRISPR-Cas12b

Along the biological studies, there exist a variety of CRISPRs discovered in many bacteria and archaea. By effector composition, modes of action, and targeted molecules, CRISPR-Cas can be categorized into two classes and six types[9]. Class 1 CRISPR requires multiple protein effectors, along with crRNA and tracrRNA, to form a functional holoenzyme. Class 2 CRISPR, on the other hand, only requires single enzyme as the sole effector to be functional, and thus receives the most attention. Currently, Cas9, the most famous class 2, type II effector, was first utilized in mammalian genome editing[10, 11] by using sgRNA in place of crRNA and tracrRNA. Particularly, the engineered sgRNA containing a complementary region (~20 bp) against the specific DNA site of the target

doi:10.6342/NTU202303502

genomes, carries a scaffolded RNA region to replace the additional tracrRNA. Subsequently, the sgRNA directs Cas9 RNP complex first to identify and induce a site-specific double strand break in the protospacer adjacent motif (PAM) near the complementary region, rendering a possible knockout on the target genome. The typical PAM of Cas9, for example, is 5'-NGG-3'[13].

Other than CRISPR-Cas9, Cas12b/C2c1 was first described in 2015[14]. Cas12b/C2c1 belongs to class 2 CRISPR/Cas, but is categorized into type V due to its activity on both DNA and RNA. Cas12b's PAM is 17-23 bp downstream of the complementary region, as opposed to being "adjacent" like Cas9's. [14]. Furthermore, the Cas12b effector exhibits a smaller size (MW: 130 kDa) in comparison to Cas9 (MW: 160 kDa), and displays a lower off-target rate and higher pH stability/resistance than Cas9[15]. AaCas12b, as described by Teng et al. (2018), works in a broad temperature range (31-79 °C) and a broad pH (3-8), making it a superior choice when confronting extreme conditions[16].

doi:10.6342/NTU202303502

1.2 CRISPR-Cas and Gene Therapy

Since the first *in vitro* work reported by Cong et al. and Mali et al., CRISPR-Cas have been intensively explored for its potential for *in vivo* applications[17]. CRISPR-Cas have been used widely for gene editing in different model organisms including fruit fly, zebrafish, and mouse[17]. Also, several disease models such as cataracts, hypercholesterolemia, HIV, were proven to be curable by CRISPR-Cas mediated gene therapy in preclinical setups[18]. Furthermore, various clinical trials of CRISPR-Cas gene therapies are currently underway toward fighting against cancers, multiple myeloma, HIV, etc.[17].

1.2.1 CRISPR-Cas Delivery

In spite of the great promises of *in vivo* CRISPR genome editing, there is a growing demand for enhanced biosafety and efficiency to address the complexity and specific delivery routes within the hosts. Before the CRISPR-Cas payload can be delivered to its destination, it must first overcome the barriers of hosts. Researchers have proposed a wide variety of approaches to improve delivery efficacy, specificity, and biosecurity[19].

doi:10.6342/NTU202303502

CRISPR-Cas cargos can be categorized according to the mode of delivery (viral, artificial polymer, liposome, physical, etc.) and the form of CRISPR-Cas (DNA, RNA, ribonucleoprotein (RNP))[19]. Direct delivery of CRISPR-Cas gene into cells of interest via viral vectors is among the most common approaches. However, viral vectors suffer from several drawbacks such as carcinogenesis and severe immune responses[20], which can inhibit their applications. Physical methods such as microinjection or electroporation are highly controllable, but challenging to implement *in vivo*[20]. Artificial nanoparticles or liposomes carrying CRISPR-Cas DNA, mRNA or RNP are free of viral risks, but their efficacy varies by cell types and tissues, and the production is relatively complicated and expensive[20].

For a successful delivery system, the form of CRISPR-Cas is also playing a crucial role. DNA encoding CRISPR-Cas gene is inexpensive and simple to synthesize, but it requires nuclear transfections, which may introduce a risk in host genome alternation and disruption. CRISPR-Cas mRNA can be directly translated within the cytosolic environments, but its preparation is rather challenging it has suffered from a limited half-life. CRISPR-Cas RNP can conduct genome editing once it has been transferred into the

doi:10.6342/NTU202303502

nucleus, however the RNP itself may induce immune responses by host's T cell[21], and there is no universal vector to deliver CRISPR-Cas RNP at present[19].

1.3 Bacterial Vectors in Cell Delivery Platform

Bacterial vectors have been used to delivery DNA since the end of last century[22]. Researchers have used intrinsically invasive strains such as *Salmonella typhimurium*[23], *Listeria monocytogenes*[24], and recombinant *Escherichia coli*[25] to deliver exogenous genes into different cell lines *in vitro*. Some of the bacteria have the ability to inhabit and thrive in the tumor tissues, mainly due to hypoxia microenvironments in tumors[26]. By this preference, these bacteria strains become a prefect option for cancer targeting[26]. Additionally, further engineering of native bacterial strains is necessary to achieve the advancement of bacterial based vehicles, with reduced non-specific toxicity (bacteremia) and immune responses to hosts[26]. Currently, researchers have rewired bacterial cells to generate attenuated and recombinant strains to minimize the immune response and other biosafety problems. For example, attenuated *Salmonella enterica* serovar Typhimurium has been used in delivering pneumococcal protein PspA to protect hosts from the infection of *Streptococcus pneumoniae*[27]. Attenuated and recombinant bacterial vectors are

doi:10.6342/NTU202303502

normally not able to proliferate in the hosts, and their immune irritation are minimized by some deletion in natural toxic genes[28].

For *Escherichia coli*, non-invasive *E. coli* K12 strain was first proven to deliver expressible exogenous genes into mammalian cells by expressing the invasin (*inv*) gene from *Yersinia pseudotuberculosis* and listeriolysin O (*hly*) from *Listeria monocytogenes*[25]. As the development of recombinant technology, researchers have increased the delivery efficiency and specificity of engineered bacterial vehicles by the addition of features like antibiotics attenuation[29], expression of lysis gene[30], or lysosomal inhibition[31].

Additionally, current strategies such as pH-low insertion peptide (pHLIP)[32] have been employed to trigger cellular entry/uptake and cargo delivery. Giacalone et al. (2006) used protoplasted *E. coli* minicells to deliver plasmid DNA into Cos-7 cell, achieving 25% of gene expression by presenting invasion domains on *E. coli*'s inner membrane[33]. Zhang et al. used EcN minicell packaged with doxorubicin and presenting pHLIP to selectively eradicate cancer cells in the hypoxic microenvironments[32]. As demonstrated,

doi:10.6342/NTU202303502

bacterial vectors can deliver various form of compounds, in addition to their programmed capacity to produce DNA, RNA and protein.

1.3.1 Probiotic *E. coli* Nissle 1917 (EcN) and delivery systems

Among various choices of bacterial vectors, *E. coli* Nissle 1917 (EcN) has a role to play in. EcN was first isolated by a physician named Alfred Nissle from a German soldier during the First World War in 1917. This soldier, who resided in a severely *Shigella*-contaminated region, didn't suffer from any intestinal disease. Nissle theorized that it is this particular strain pf bacteria, EcN, was that shielded the soldier from acquiring *Shigella*[34]. During 1980s, scientists started to examine the biosafety issue of EcN. EcN was later confirmed to be non-pathogenic, and also showed strong antagonistic activity toward pathogenic microorganisms by immunomodulation, anti-inflammation, and direct inhibition on the invasive microorganisms[34]. Microcins, a type of bacteriocin, produced by EcN can combat pathogenic bacteria such as *Pseudomonas aeruginosa* or *Salmonella*. In addition, EcN can induce defensin 2 in intestinal epithelium cells to prevent pathogen attachment[35].

doi:10.6342/NTU202303502

Beside its intrinsic ability as a probiotic, recombinant EcN strains were constructed for specific aims, called EcN therapies. Researchers designed EcN to specifically target and destroy pathogens like nontyphoidal *Salmonella,* cure hyperammonemia by the production of ArgR protein, or treat cancer by exploiting the hypoxia-tropic nature of the microbe[35]. EcN vehicles with cytotoxic agents such as colibactin[36], azurin[37], or prodrugs such as CB1954, 5-FC and fludarabine phosphate were also demonstrated to be successful in treating cancers[38].

Additionally, EcN have been used intensively as delivery platform for DNA, RNA and drugs and bioengineering strategies have been employed to create advance EcN vehicles with tailored functionalities. For instance, type III secretion system[39] or invasin[25] can empower those non-invasive EcN to deliver cargos intracellularly.

1.3.2 Minicells as Delivery Platform

Currently, among various bacterial vectors, minicells derived from engineered bacteria strains were proposed in order to increase the biosafety and to diminish the interference of bacterial genome. Minicells are miniature anucleate cells derived from

doi:10.6342/NTU202303502

abnormal, asymmetric cell division[40]. The Z-ring normally accumulates at the middle of a bacteria cell when dividing. However, the mutation of middle-localizing genes *minCDE* or overproduction of Z-ring gene *ftsZ* can lead to abnormal division not only at the middle of the cell but also at the two poles. Once the division ended at two poles of the bacterial cell, anucleate minicells are formed[41]. A minicell retains cellular activity such as transcription, translation, and other enzymatic activity, but is unable to divide anymore[41].

Due to the defect on proliferation, minicells are safer than attenuated bacteria as the delivery system[42]. Several groups have shown the potential in using minicells as a delivery platform[32, 43-45]. To minimize the immune response, probiotic *E. coli* Nissle 1917, already used in medical therapy[46], is preferred to be used. Therefore, it is our goal to delivery CRISPR-Cas by *E. coli* Nissle 1917-derived minicells. To our knowledge, there is currently no research on the CRISPR-Cas delivery by bacterial vectors. The feasibility and utility are yet to be fully explored.

1.4 Specific Aims

doi:10.6342/NTU202303502

In this research, we use AaCas12b, with a small, highly thermostable and acid-tolerant CRISPR RNP as the cargo to be delivered. AaCas12b has be reported for its mammalian cell genome editing with high efficiency and low off-target rate[16]. In order to minimize the biosafety concern, we utilize the probiotic *E. coli* strain EcN and its derivative non-proliferating minicells as the delivery platform. Cas12b and the sgRNA were first produced in EcN minicells, and then be delivered into mammalian cells with the assist of invasin and listeriolysin O, in order to bind to cellular surface and to escape from the endosome. We first demonstrated that the minicells can produce corresponding recombinant protein as functional cargos. Later, we ensured the delivery of cargos to the cytosolic environments of target cells by expressing *inv* and *hly*. Finally, the delivery efficiency of this platform was depicted along with subsequent pre-treatment steps for enhanced editing efficiency (~5%).

doi:10.6342/NTU202303502

2. Materials and Methods

2.1 Plasmid, Bacteria Strain and Mammalian Cell Line

2.1.1. Bacterial Strains

Plasmids and bacteria strains are detailed in Table 1. Reporter protein (mCherry), genome editor (Cas12b), were constructed into pACYC plasmid after T5 constitutive promoter with *lacO* operator. Single guide RNA was constructed into the same plasmid of Cas12b under J23119 constitutive promoter with chloramphenicol resistance. *Yersinia pseudotuberculosis* invasin gene (*inv*) and *Listeria monocytogenes* listeriolysin O gene (*hly*) were constructed into pGB2 plasmid with streptomycin resistance. Most plasmids, if not mentioned, were constructed by senior students.

Escherichia coli Nissle 1917 (EcN) was bought from Germany. Minicell strain (EcN mini) was originated from *E. coli* Nissle 1917 with the knockout on *minCD* gene and *recA* gene. Overnight incubation showed the production of minicell. *DapA recA* double-knockout (EcN rd-) strain was produced by senior students.

doi:10.6342/NTU202303502

2.1.2 Cell Lines

A549 and HeLa used in the experiment for cell editing assay, transfection, and transduction were all cultured in DMEM with 10% fetal bovine serum (Invitrogen™). DGG.HeLa monoclone was produced and selected through stable transfection by Lipofectamine 3000 (Invitrogen™) and G418.

2.1.3 Plasmids and Primers

For CRISPR editing, AaCas12b gene sequence was cloned into pACYC2 under the expression and control of T5 promoter and lacO. The single guide RNA was expressed by J23119 promoter.

For cellular tracking, mCherry red fluorescence protein was cloned into pACYC2 under the expression and control of T5 promoter and lacO.

doi:10.6342/NTU202303502

For delivery and cellular entry, *inv* gene from *Yersinia pseudotuberculosis* and *hly* from *Listeria monocytogenes* was cloned into the arabinose-induced pBAD plasmid (only *hly* was inducible), and pGB2 low copy plasmid with the SC101 origin. pGB2-inv-hly' indicated that the secretional peptide of LLO was eliminated.

For mammalian cell editing reporter, DsRed-eGFP'-eGFP'' (DGG) reporter cassette was constructed into pLAS3w.PNEO lentivector under the control of CAG promoter. The other information is provided in Table 1 and in the appendix.

Table 1. Plasmids and strains used in this research, its abbreviation, and its description.

Plasmid name	Abbreviation	Description
pACYC2-T5lacO-Cas12b-3NLS-sgEGFP8	p12E8	Overexpress Cas12b and single guide RNA targeting *egfp*
pACYC2-T5lacO-Cas12b-3NLS-sgSpacer	p12SP	Overexpress Cas12b and single guide RNA targeting *Spacer*
pACYC2-T5lacO-Cas12b-3NLS-sgControl	p12NC	Overexpress Cas12b and single guide RNA without any target

doi:10.6342/NTU202303502

pACYC2-T5lacO-mCherry	pT5RF	Overexpress mCherry recombinant protein
pBAD-inv-hly	pBAD	Express *Y. pseudotuberculosis* invasin and an inducible *L. monocytogenes* listeriolysin O controlled by arabinose
pGB2-inv-hly	pGB2	Express *Y. pseudotuberculosis* invasin and *L. monocytogenes* listeriolysin O
pGB2-inv-hly’	pGB2’	Express *Y. pseudotuberculosis* invasin and *L. monocytogenes* listeriolysin O without its secretion signal
pLAS3w.DsRed-eGFP’-eGFP’’	pDGG	Lentivector encoding DsRed-eGFP-eGFP gene cassette for transduction
E. coli Nissle 1917, wildtype	EcN	Wildtype *E. coli* Nissle 1917
E. coli Nissle 1917 *minCD- recA-*	EcN mini	*E. coli* Nissle 1917 with *minC* and *minD* and *recA* genes knockout

doi:10.6342/NTU202303502

E. coli Nissle 1917 *dapA- recA-*	EcN rd-	*E. coli* Nissle 1917 with *dapA* and *recA* genes knockout, diaminoheptanedioic acid auxotrophic
HeLa with pLAS3w.DsRed-eGFP'-eGFP''	DGG.HeLa	Stable single clone of HeLa cells transfected with pDGG, with a gain-of-function CRISPR-reporting cassette

2.2 Culture Medium and Other Reagents

2.2.1 Bacterial Medium and Drugs

Luria-Bertani broth (LB): 2.5 g LB powder (Cyrusbioscience) was dissolved in 100 mL dH_2O, autoclaved at 121°C for 20 minutes.

LB agar plate: 1.5% Bacto agar (Cyrusbioscience) was added to prepared LB medium. After autoclavation and cool-down to 50°C, the agar was poured into 90 mm petri dishes.

Brain heart infusion broth (BHI): 3.7 g BHI powder (BD) was dissolved in 100 mL dH_2O, autoclaved at 121°C for 20 minutes.

doi:10.6342/NTU202303502

Brain heart infusion agar plate: 1.5% Bacto agar (Cyrusbioscience) was added to prepared BHI medium. After autoclavation and cool-down to 50°C, the agar was poured into 90 mm petri dishes.

Streptomycin stock solution (100 mg/mL): 100 mg streptomycin sulfate (Sigma) was dissolved in 1 mL dH_2O, filtered by 0.20 μm CA filter, and stored at -20°C.

Kanamycin stock solution (50 mg/mL): 50 mg kanamycin sulfate (USP) was dissolved in 1 mL dH_2O, filtered by 0.20 μm CA filter, and stored at -20°C.

Chloramphenicol stock solution (35 mg/mL): 350 mg chloramphenicol (Sigma) was dissolved in 10 mL 100% ethanol, filtered by 0.20 μm CA filter, and stored at -20°C.

Ceftriaxone stock solution (100 mg/mL): 100 mg of ceftriaxone disodium salt hemiheptahydrate (TCI) was dissolved in 1 mL dH_2O, filtered by 0.20 μm CA filter, and stored at -20°C.

Tetracycline stock solution (100 mg/mL): 1000 mg tetracycline hydrochloride (Sigma) was dissolved in 10 mL 100% ethanol, filtered by 0.20 μm CA filter, and stored at -20°C.

Ampicillin stock solution (100 mg/mL): 100 mg ampicillin sulfate (Sigma) was dissolved in 1 mL dH_2O, filtered by 0.20 μm CA filter, and stored at -20°C.

Penicillin G stock solution (100 mg/mL): 100 mg penicillin G (Sigma) was dissolved in 1 mL dH_2O, filtered by 0.20 μm CA filter, and stored at -20°C.

doi:10.6342/NTU202303502

1M Tris-HCl (pH 8.0) stock solution: 121.1 g tris base was dissolved in 800 mL of Milli-Q water, the pH was adjusted by 6N HCl drop by drop until it reached 8. The volume was adjusted to 1000 mL, and autoclaved at 121°C for 20 minutes.

Hen egg white lysozyme stock solution (10 mg/mL): 100 mg of hen egg white lysozyme (Cyrusbioscience) was dissolved in 10 mL of sterile 50 mM tris buffer, filtered by 0.20 μm CA filter, and stored at 4°C for no more than one month.

Polymyxin B stock solution (10 mg/mL): 10 mg of polymyxin B sulfate (Sigma) was dissolved in 1 mL sterile Milli-Q water, and stored at 4°C for no more than one month.

2.2.2 Cell Culturing Medium and Drugs

Fetal bovine serum (FBS): from Gibco 10438026, stored at -20°C

DMEM (10% FBS): Dulbecco's Modified Eagle Medium (Gibco) powder was dissolved in 1000 mL Milli-Q water, 3.7 g sodium bicarbonate was added, and the solution was filtered by 0.20 μm CA filter. 10% FBS was added before storage at 4°C.

Trypsin solution: 0.25% trypsin-EDTA (1x) (Gibco)

DPBS: Dulbecco's phosphate buffer saline (Gibco), stored at room temperature.

G418 (50 mg/mL): geneticin solution (Gibco), stored at 4°C or -20°C.

doi:10.6342/NTU202303502

Gentamycin (10 mg/mL): gentamycin solution (Gibco), stored at 4°C.

Streptomycin and Penicillin G solution: from Gibco, stored at 4°C

Paraformaldehyde solution (1% or 4%): 0.5 g or 2.0 g of paraformaldehyde (Sigma) was added to 1x PBS with gentle stirring and heating (~60°C). To enhance dissolution, few drops of 6N NaOH solution was added to the solution. The pH was examined by litmus paper to ensure that the pH ranges from 6-8. The solution was stored at -20°C.

Quinacrine solution (10 mg/mL): 10 mg of quinacrine was dissolved in sterile DPBS and stored at 4°C. When staining, the solution was diluted in DPBS or growth medium at a ratio of 1:2500.

2.3 Plasmid Construction and Transformation

2.3.1 pACYC-T5-mCherry (pT5RF)

Gene sequence of mCherry was amplified by PCR with the addition of overlapping region of pACYC2 MCF, and was further inserted to pACYC2 with its T7 promoter replaced with a T5 promoter by Gibson assembly.

2.3.2 pLAS3w.DsRed-eGFP'-eGFP".WPRE (DGG(WPRE))

doi:10.6342/NTU202303502

Cassette of DsRed-eGFP'-eGFP'' (DGG) was produced by senior students. DGG sequence was amplified by PCR with the overlapping region of pLAS3w backbone as well as WPRE 5' sequence. WPRE sequence was amplified from plasmid pLAS3w backbone. DGG, WPRE and pLAS3w backbone was assembled by Gibson assembly.

2.3.3 Preparation of Electrocompetent Cell and Electroporation

EcN mini with/without harboring plasmid was inoculated in 4 mL BHI medium with/without antibiotics, and was cultured at 30°C for 16-18 hours. The next day, 1 mL of overnight culture was inoculated into 100 mL BHI medium and further incubated at 30°C with 250 rpm shaking. As soon as the reading of OD_{600} reaches 0.3-0.5, the culture was transferred to falcon tubes precooled on ice. Bacterial cells were pelleted by 4000g, 10 minutes at 4°C, washed by cold Milli-Q water thrice, and finally re-suspended in 1 mL of cold 10% glycerol (in Milli-Q water). The suspension was dispersed into eppendorf and stored at -80°C until usage.

For electroporation, pre-made electrocompetent cells were thawed on ice, and 1-2 μL of plasmid (10-100 μg) was added to the suspension as soon as it thawed. The

doi:10.6342/NTU202303502

suspension was transferred into a 0.1 mm Gap cuvette (BTX), and pulsed (1.5 kV, 200, 25 μF) by Electro Cell Manipulator ECM630 Electroporation System (BTX). After the pulse, bacterial cells were immediately re-suspended in 1 mL BHI without any antibiotics. Let the culture recover at 30°C for 1-16 hours. The recovered culture was plated into corresponding plates.

2.3.4 Development of DGG.HeLa Stable Cell Line

To prepare a stable cell line, 5 μg of DGG plasmid was transfected to HeLa cell line by lipofectamine 3000 following the manufacturer's manual. 48 hours post-transfection, cells were separated into three individual 6-wells with DMEM (10% FBS) supplied with 700 μg/mL G418. 1-2 weeks, outgrowth of stably expressing colonies could be observed under fluorescence microscopy. *In situ* trypsinization was conducted in the sites full of stably expressing colonies. The trypsinized mixture was seeded to a 48-well plate.

To obtain a single clone, stable clones were outgrowing until confluency at a T-25 plate. Cells were trypsinized and diluted to 10 cells/mL. The mixture was spread into 96-well (100 μL/well indicating 1 cell/well) under the selection of G418 (700 μg/mL). The

doi:10.6342/NTU202303502

outgrowth could be observed 2 weeks after seeding. Positive stable single clones were expanded until confluency at 100 mm plate and were froze in liquid nitrogen.

2.4 Production and Purification of Cas12b RNP in Minicell

Cas12b were overexpressed by EcN, or EcN mini by the following process: bacteria culture was inoculated into 4 mL of BHI broth with appropriate antibiotics and incubated overnight at 37°C, 250 rpm. The next day, overnight saturated culture was inoculated into 100 mL BHI with proper antibiotics, and further incubated at 37°C, 250 rpm until OD600 reaches 0.4-0.6. 1mM IPTG was added to the culture to induce the production of mCherry or Cas12b. The induction step was conducted at 25°C, 250 rpm for 18 hours.

2.4.1 Purification of Cas12b RNP

For the purification of Cas12b RNP, induced culture was spun down at 13000g for 20 minutes, and washed by 50 mM Tris-HCl (pH 8.0). The pellet was re-suspended in 30 mM imidazole in 50 mM Tris-HCl (pH 8.0) before at the concentration of 1 g/10 mL and with the supplement of 500 ug/mL hen egg white lysozyme. The suspension was sonicated (3 s pulse, 5 s stop, 15 minutes total, 60% amplitude) and clarified by spinning

doi:10.6342/NTU202303502

at 6000g for 10 minutes, passing through 0.45 and 0.20-μm CA filter (Satorius^{TM}). Lysate was incubated at 4°C overnight with the addition of Ni-NTA agarose beads (1 mL/10 mL) to induce sufficient binding. The next day, agarose beads were packed, and washed by 5x column volume of 30 mM-, 50 mM-, 100 mM-imidazole in 50 mM Tris-HCl (pH 8.0). Cas12b RNP was eluded by 10 mL of 500 mM imidazole in 50 mM Tris-HCl (pH 8.0). The eluent was concentrated and the buffer was replaced to desired ones by Amicon Ultracentrifuge tubes (100 kDa cut-off). For lipofection and nucleofection, Cas12b RNP was stored at 50 mM Tris-HCl (pH 8.0) at 4°C for no more than one week. For *in vitro* DNA cleavage, Cas12b RNP was stored at a storage buffer (50mM Tris-HCl, 200mM KCl, 1mM DTT, 20% glycerol) at -80°C. The concentration was quantified by Bradford method, with bovine serum albumin as the standard.

For minicell portion of protein, the induced culture was first centrifuged at 2000g for 20 minutes to get rid of the majority of large, parental cells. The rest of minicells were gathered through the process mentioned above.

doi:10.6342/NTU202303502

2.4.2 SDS-PAGE

EcN cell/minicell lysate as well as purified Cas12b RNP were examined by 6% SDS-PAGE. For whole-cell lysate, OD_{600} = 0.2 of EcN cell/minicell was pelleted, and re-suspended in TE buffer with protein loading dye. For purified Cas12b RNP, 1~3 mg of RNP was diluted by TE buffer and protein loading dye. The gel was stained with Coomassie blue R to check the expression of recombinant proteins.

2.4.3 *In vitro* DNA Cleavage Test

The substrate dsDNA was amplified by Q5 DNA polymerase (New England Biolab™) and purified by DNA gel clean up kit (Zymo™). In a typical reaction, 1 μM of Cas12b RNP and 300 ng of dsDNA were added to NEB buffer 2, incubated at 37°C for 2 hours, and quenched by adding proteinase K and RNase A.

The results were examined by 3% TAE agarose gel electrophoresis, pre-stained with Safeview (abm™).

doi:10.6342/NTU202303502

2.5 Production and Purification of Minicell

Saturated culture of EcN mini was used for minicell purification, modified from a previous report [47]: the culture was centrifuged at 2000g for 20 min to remove the majority of the parental cell. The supernatant was further centrifuged at 13000g for 30 min to gather all residual bacteria and minicell. Fresh medium without antibiotics was used to resuspend the pellet. The resuspended culture was first incubated at 37°C, 250 rpm for about 1 h to facilitate proliferation of parental cell. Later, antibiotic cocktail (ceftriaxone 100 μg/mL, penicillin G 100 μg/mL, kanamycin 50 μg/mL) was added to kill the growing bacteria for 1 h, and further incubate at 4°C overnight to kill the slow-growing bacteria. Low speed spinning at 800g for 15 min is used to eliminate dead large cell and cell debris. The supernatant is clarified by passing through a 0.80 μm filter (Satorius^{TM}).

Purified minicell was gathered by centrifugation (13000g, 30 min) and resuspended in desired buffer, measured by OD_{600} to quantify the concentration.

doi:10.6342/NTU202303502

2.5.1 Quantification of Minicell

Purified minicell was diluted to different OD_{600} (1-0.5) in 1 mL deionized water, span down, and frozen-dried by a typical protocol. The dried pellets were weighted and the relation between OD_{600} and the dry weight was obtained by simple linear regression.

The dry weight of minicell was divided with total dry weight (minicell + dead cell + parental cell from upstream purification steps) to obtained the yield.

2.5.2 Determination of Contamination from Parental Cell

1 mL of purified minicells and samples from each purification step were gathered, and diluted into 1x, 0.1x, or 0.01x. Bacterial cells were span down to remove residual antibiotics within the medium, and were re-suspended in 1x PBS. To determine the contamination, BHI agar plates with the addition of chloramphenicol (12.5 μg/mL) with/without streptomycin (50 μg/mL) were inoculated with the bacterial suspension, and were incubated at 37°C overnight. Colony forming unit (CFU) per plate and volume were calculated.

doi:10.6342/NTU202303502

2.5.3 Growth Curve of EcN mini and EcN WT

EcN mini and EcN wildtype (WT) were inoculated from the frozen stock into 5 mL BHI medium starter culture and incubated at 37°C, 250 rpm for 18 hours. The next day, 1% (0.5 mL) of overnight cultures were inoculated to antibiotic-free fresh BHI medium (50 mL) in flasks and were incubated at 37°C, 250 rpm for 1 hours. The optical density at 600 nm was sampled each hour (0-10 hours).

2.5.4 Microscopy

Purified minicells (EcN mini T5RF) and samples from each purification step were diluted in 1x PBS and were observed under fluorescence microscopy and 1000x oil lenses. The ratio of minicell to parental cell and the size of minicell were examined.

2.6 Cell Culture and Minicell Co-Incubation Test

2.6.1 Cell Viability Test

doi:10.6342/NTU202303502

HeLa, A549 cells were seeded into 96-well plate with the number of 5000 cell per well one day before the test. The next day, old medium was replaced with fresh medium before coincubation with minicell.

Purified minicell and parental cell and EcN rd- are quantified by OD_{600} and were transformed into counting by the published work[33]. In short, OD_{600} =1 indicates $5*10^{10}$ minicell/mL or $8*10^{8}$ bacteria/mL within the solution. Minicell and parental cell were resuspended in DPBS with the final OD_{600} = 1.

To test the toxicity of minicell toward each cell line, different bacteria-to-cell ratio (B/C ratio) of minicell and parental cell, with or without antibiotics addition (penicillin G, 100 μg/mL), were added to the medium and co-incubated overnight. The next day, old medium was discarded and each well was rinsed with DPBS thrice. LIVE/DEAD staining (Invitrogen™) was used to test the relative death or relative alive of each group. Each group was conducted in triplet.

doi:10.6342/NTU202303502

2.6.2 Minicell Delivery Test

HeLa, A549 cells were seeded into 24- or 6-well plate with appropriate number one day before the test. The next day, old medium was replaced with fresh medium before co-incubation with minicell.

Purified minicell with mCherry as labels was added to each well with the desired B/C to co-incubate with the cell. 30 minutes, 1 hour or 2 hours after the addition, the medium was replaced with sterile medium w/wo antibiotics. To examine the invasion efficiency, each well was examined under fluorescence microscopy at 0, 2, 4, 6, 12, 24, 48 hours post co-incubation.

2.6.3 Lysozyme Treatment

To test the effect of lysozyme, purified minicells were re-suspended in 50 mM Tris-HCl (pH 8.0) with the supplement of 8% sucrose, to prevent possible osmotic stress and cell lysis. Hen egg white lysozyme with the final concentration of 1000, 500, 100, 50 μg/mL was added to the minicell suspension, incubated at a 37°C water bath for 0, 1, 5,

doi:10.6342/NTU202303502

10, 20, 60, 120 minutes, respectively. After all, the minicell suspension of B/C 2000 was added to HeLa cell pre-cultured in a 24-well plate, and further co-incubate for 2 hours. The old medium was later discarded and washed with DPBS thrice, and fresh medium supplied with 20 μg/mL gentamycin was added for subsequent culturing.

2.6.4 Lysozyme and Polymyxin B Treatment

To test the synergistic effect of lysozyme and polymyxin B, purified minicells were re-suspended in the isosmotic buffer described before. Polymyxin B in the concentration of 0, 10, 25, 50 μg/mL with/without 500 μg/mL lysozyme was added to the minicell suspension, and was incubated at 37°C for 30, 60, 120 minutes, respectively. The suspension was added to HeLa cell pre-culture in a 24-well plate with the B/C of 2000, co-incubated for 1.5 hours, and final discarded and replaced with fresh medium.

Each well was observed directly after the replacement, or 24-hour post exposure to minicell, under fluorescence microscopy.

doi:10.6342/NTU202303502

2.6.5 Immunofluorescence Staining

Before fixation, cells were washed by DPBS three times. Cells were then fixed by 4% paraformaldehyde in DPBS (pH 7.4) for 15 minutes at room temperature. To permeabilized the cell, 0.1% Triton X-100 in DPBS was selectively added and DPBS was added to the control group (non-permeabilized). Each well was blocked by 1% BSA (in DPBS) for 1 hour at room temperature. Primary antibody against *E. coli* (rabbit, Abcam™) or anti-His (rabbit, Bioman) with the dilution ratio of 1:500 was used to target minicell or delivered protein at room temperature for 2 hours or at 4°C overnight. Secondary antibody (anti-rabbit IgG, Abcam™) labeled with Alexa-488 and was diluted to 1:1000 in order to stain the minicell at room temperature for 1 hour away from light. The cells were washed with DPBS thrice between each step. For nucleus staining, 0.02 μM Hoechst 33342 (Bio-Rad™) was added to the sample, staining for 10 minutes, and washed away before observation.

doi:10.6342/NTU202303502

2.6.6. Transfection of Cas12b RNP by Lipofection

DGG.HeLa cells were seeded into 24-well in a number of 100,000 per well one day before transfection. The next day, purified Cas12b RNP was thawed, and was added to 50 μL Opti-MEM with 2 μL of Lipofectamine 3000 reagent in different amount (0, 125, 250, 500, 1000, 2000 ng), let incubate at room temperature for 15 minutes. After the incubation, the mixture was dispersed evenly to each well, pre-replaced with fresh DMEM (10% FBS) supplied with 500 μg/mL G418. 48 hours later, each well was observed individually under fluorescence microscopy.

2.6.7 Transfection of Cas12b RNP by Electroporation

DGG.HeLa cells were seeded to 100 mm plate until confluency. Confluent cells were trypsinized and re-suspended in a concentration of 10^7 cells/mL in Opti-MEM. The electroporation process was conducted by BTX ECM 630 in the following configuration: 100 V (LV), 200 μF, no resistance. 40 μL of cells ($4*10^5$ cells) were mixed with different concentration of purified Cas12b RNP (5, 10, 20, 30 μg) or BSA (10 μg) and the mixture was added to a 1 mm gap BTX disposable cuvette. After electroporation, the mixture was

doi:10.6342/NTU202303502

re-suspended immediately with 200 μL of Opti-MEM and was seeded to 1 mL DMEM (10% FBS) supplied with 500 μg/mL G418 in a 6-well plate. 24-48 hours later, each well was observed individually under fluorescence microscopy.

doi:10.6342/NTU202303502

3. Results

3.1 Minicell Construction and Protein Production

3.1.1 Clarification of Minicell-Producing Strain EcN mini

The *recA minCD*-knockout *E. coli* Nissle strain (EcN mini) was constructed previously by former members in the lab using lambda phage recombination methods [48]. *minC/minD* are responsible for modulating the mid-cell localization by concentration oscillations. Knocking out *minC* and *minD* would lead to an abnormal centralization of cell-separating Z-ring and inconsistent sizes of daughter cells. (Figure 1A). Upon the aberrant bacterial cell division, the smaller daughter cell will contain no chromosome DNA, while the other will contain two copies. Theoretically, the diploid daughter cell can further proliferate to produce two normal daughter cells or one normal cell and one minicell. To probe the growing condition of EcN mini, we cultured it in LB medium or BHI medium, checking the overnight optical density, as compared to wildtype EcN.

doi:10.6342/NTU202303502

EcN mini grew normally in both LB medium and BHI medium. We plotted the growth curve of EcN mini and WT within 10 hours at 37°C, 250 rpm (Figure 1B). With the same initial seeding OD_{600} (0.113), EcN mini had a lower OD_{600} throughout the test. Although the lower OD_{600}, the doubling time of EcN mini and WT were identical (~37 minutes), showing no deficiency in normal cell proliferation. This may due to the distinct nature of optical absorption between minicells and regular-sized cells, as minicells were about 1/4 or less the size of regular cells[47]. To test the morphology of EcN mini's minicells, EcN mini was transformed by electroporation with plasmid pT5RF, which can induce mCherry production with IPTG induction. Fluorescence microscopic results showed that both normal cells, longer cells, and round minicells (Figure 1C) were presented in the induced culture medium. The size of minicell majorly ranged from 0.6-0.9 μm in diameter (Figure 1D) as determined under the fluorescence microscope. The red fluorescence indicated that the round minicells was originated from EcN mini parental cells.

doi:10.6342/NTU202303502

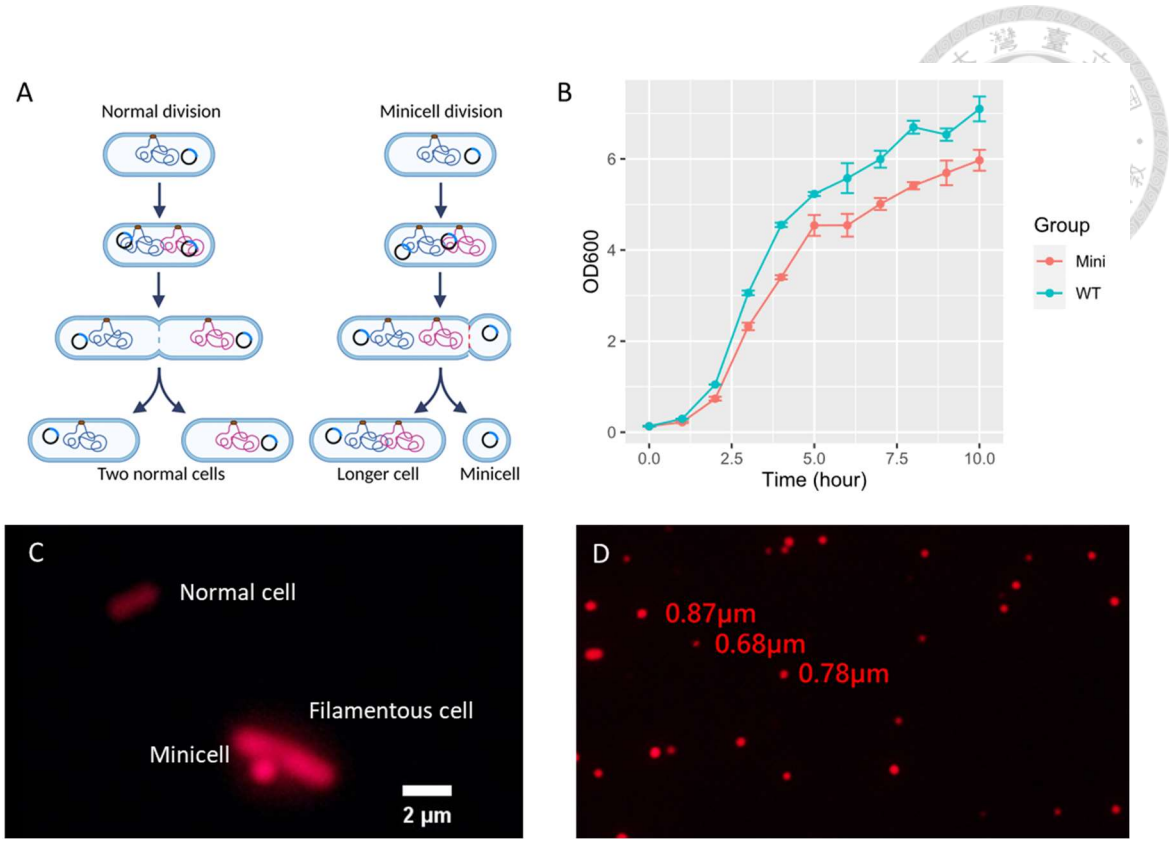

Figure 1. EcN mini and the produced minicells. **A)** Schematic diagram of minicell production from the parental cells. **B)** Growth curve of EcN min (Mini) and EcN wildtype (WT) strains. **C)** The morphology of normal, filamentous, and minicell under the fluorescence microscopy. **D)** Purified minicells with varied sizes. Scale bar = 2 μm.

3.1.2 Purification and Quantification of Minicells

The size of minicells are smaller than their parental cells, indicating that they can be physically separated from parental cells. The schematic flowchart of minicell purification was depicted in Figure 2A: Step one, the majority population of minicell was extracted

doi:10.6342/NTU202303502

through differential centrifugation (at 2000g for 20 minutes first, then at 13000g for 30 minutes). About 90% of bacterial cells were minicells after the differential centrifugation (Figure 2C) as compared to original population (Figure 2B). Step two, the gathered pellet was re-cultured in antibiotic-free fresh medium for 1 hour at 37°C to resume cell growth. Later, antibiotic cocktail (ceftriaxone 100 μg/mL, penicillin G 100 μg/mL, kanamycin 50 μg/mL) was added to the medium, followed by 37°C incubation for 1 hour, and then at 4°C overnight incubation to kill both progenitor and dormant parental cells. Ceftriaxone and penicillin G act to inhibit cell wall synthesis and kanamycin inhibit protein synthesis in growing cells. Afterwards, the dead cell debris was span down by low-speed centrifugation. 99% of remaining cells were minicells (Figure 2D). Step three, to reach a sample with higher purity, the supernatant was filtered by a 0.80 μm syringe filter to obtain a 100% minicell suspension (Figure 2E). From a typical 100 mL flask cultivation, we could obtain 0.00167 ± 0.0004g dry cell weight of minicell from 0.1846 ± 0.0296g total dry cell weight, approximately $0.886 \pm 0.0008\%$ in total culture.

To check the colony forming unit after each purification step, the pellets after each centrifugation were re-suspended in equal amount of PBS (0.1 mL), and plated on BHI agar plates. Table 2 revealed that the effective colony forming unit decreased with the

doi:10.6342/NTU202303502

purification steps. The supernatant after antibiotic cocktail treatment resulted in less than 1 CFU/mL, and 0.80 μm filtration fully eliminated the effective cell remnants. However, filtration would cause nearly ~50% reduction of total OD_{600} absorption. In the following experiments, the final minicell suspension without the filtration process was utilized upon protein purification, and filtered minicells were used for cell-related processes.

We further examined the relation between measured OD_{600} (1 mL volume) of purified minicells and its dry cell weight. The measured weight was proportional toward the measured OD_{600} (1 mL), with a linear regression function: $\mathrm{y\,(dry\ cell\ weight)} = 0.0015x\ (OD_{600}) - 0.0005, R^2 = 0.962$. Approximately, 1 mL of OD_{600} purified minicells accounted for 0.001g of frozen-dried minicells.

Table 2. Colony forming unit after each purification step. Original: original culture. Step 1: the pellet span down at 13000 g after 2000 g centrifugation. Step 2: the pellet span down after antibiotics treatment. Step 3: the pellet after 0.80 μm filtration.

	Original	**Step 1**	**Step 2**	**Step 3**
CFU/mL	Too numerous to count	21 ± 18	4 ± 3	0

doi:10.6342/NTU202303502

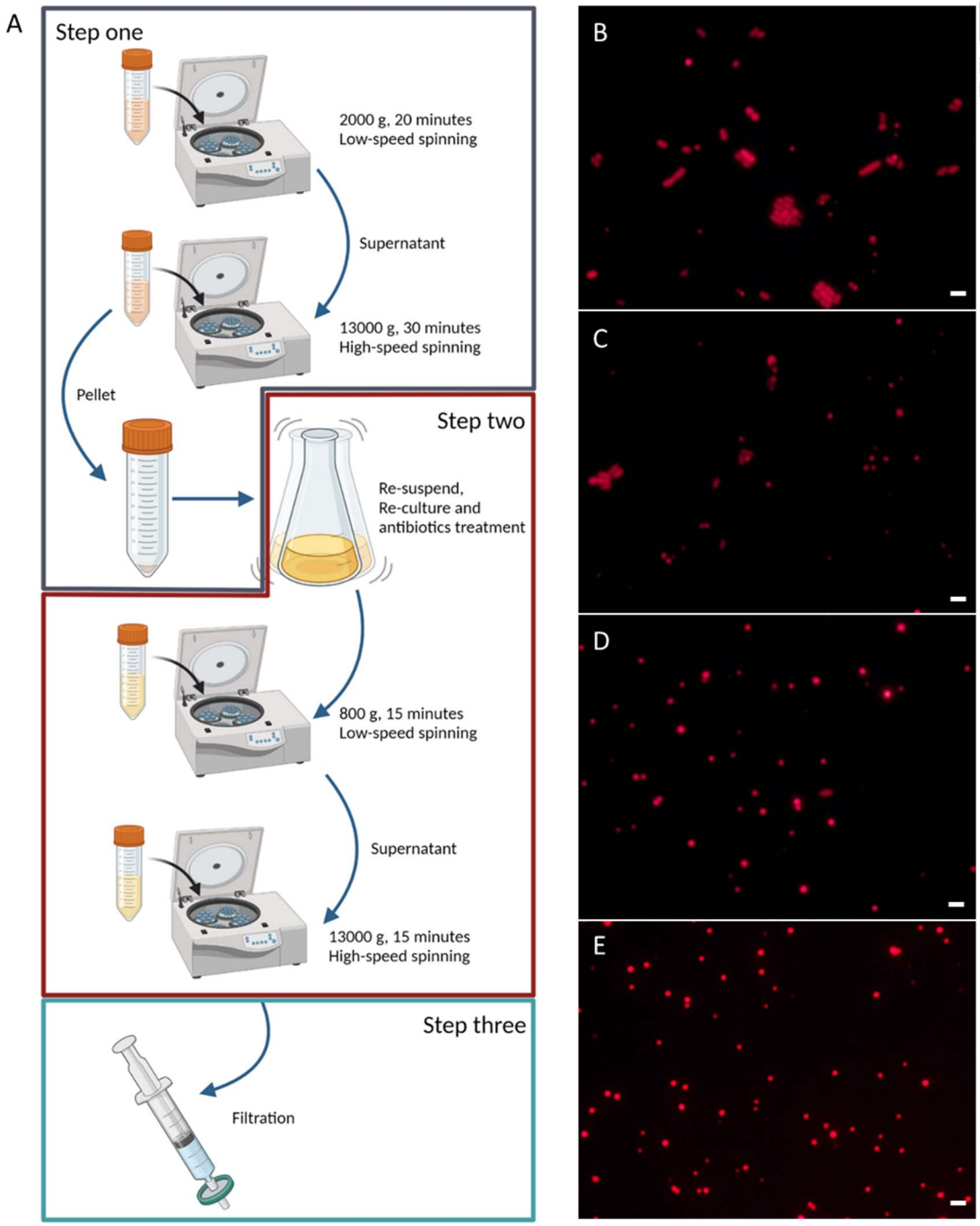

Figure 2. Establishment of minicell separation protocols. **A)** The schematic flowchart of minicell purification. **B)** The original culture (mixture of parental and minicells). **C)** After the differential centrifugation (step one), 90% of the population is minicell. **D)** After the

doi:10.6342/NTU202303502

antibiotics cocktail and the removal of dead cell debris (step two), 99% of the population is minicell. **E)** After a 0.80μm filtration (step three), 100% of the population is minicell. Scale bar = 2 μm.

3.1.3 Production of Cas12b RNP in Minicell

Previous data showed that EcN mini could successfully accumulate or produce mCherry within the minicells. We further evaluated whether a larger recombinant protein Cas12b and its accompanying sgRNA could also be presented in minicells. Briefly, EcN mini was electroporated with plasmid p12Sp and p12E8 (Appendix Table 3) and was induced with IPTG to overexpress Cas12b and sgRNA. Minicells from the induced EcN mini culture were isolated as previously described. Subsequently, minicells were lysed by a sonicator and further protein purification was carried out by the his-tagged protein purification processes [49]. Purified Cas12b RNP was stored in Tris-HCl buffer (50 mM, pH 8.0) at 4°C for no more than 2 days or at -80°C for longer storage (Figure 3A).

As the results of SDS-PAGE indicated, purified minicells contained an enhanced protein product band near 130 kDa (equivalent to the theoretical MW of Cas12b) only after IPTG induction (Figure 3B), and the his-tag purified product showed a clear single

doi:10.6342/NTU202303502

band on the gel (also ~ 130 kDa). The incubation at 37°C, 30°C, and 25°C successfully induced Cas12b production. The activity of Cas12b RNP was assayed by *in vitro* cleavage assay toward DNA fragment DsRed-spacer-EGFP (Figure 3C). It showed a complete cleavage (product size) after 2 hours of incubation at 37°C in sgEGFP (targeting *EGFP* C-terminal sequence) group, and ~50% cleavage in sgSpacer (targeting the spacer sequence between *DsRed* and *EGFP*) group, indicating that the Cas12b RNP within the minicells were functional. Different sgRNA sequences resulted in distinct cleavage patterns, indicating a specific cleavage activity by Cas12b.

doi:10.6342/NTU202303502

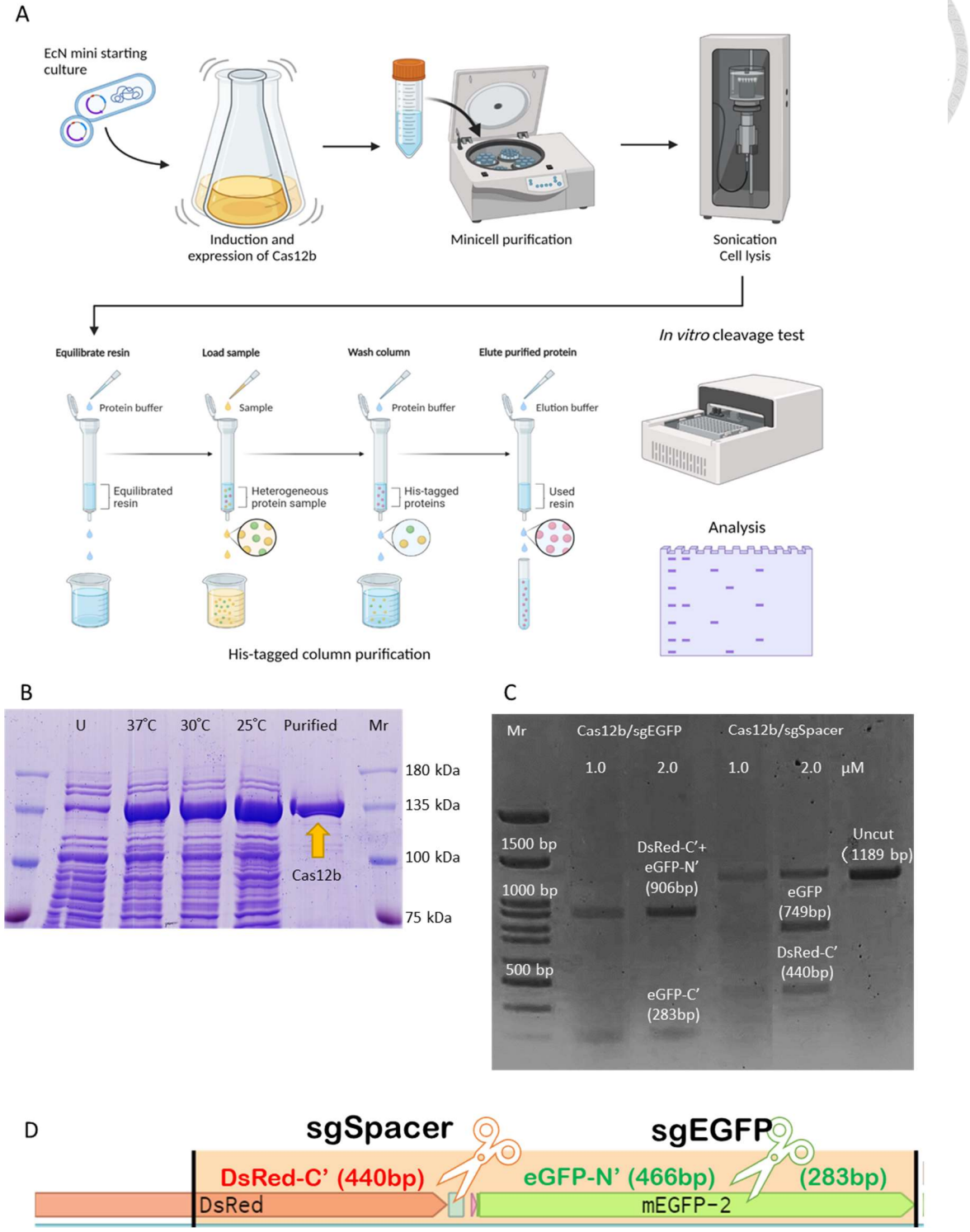

Figure 3. Cas12b RNP purification and in vitro DNA cleavage activity test. **A)** Production and purification of Cas12b RNP from EcN mini. **B)** AaCas12b (~130 kDa) showed deep

doi:10.6342/NTU202303502

band at ~130 kDa only when the culture was induced with IPTG. **C)** Activity test toward two different targets (EGFP and Spacer) on one dsDNA sequence (uncut, ~1400 bp). Mr: marker (protein/dsDNA), U: uninduced culture. D) Scheme of cut dsDNA and the fragment size.

doi:10.6342/NTU202303502

3.2 Minicells on Cell Culture

3.2.1 Cytotoxicity of Minicells

In this experiment, we aimed to figure out whether EcN-derived minicells could cause toxicity toward mammalian cells during co-cultivations. Therefore, we co-incubated purified minicells with two separated mammalian cancer cell lines, HeLa and A549 at B/C ratio of 100, 1000, and 10000 for overnight (~18 hours). Bacteria-to-cell ratio (B/C) here indicates the ratio of minicell number and cell number in the co-incubation step. In comparison, unpurified EcN mini parental cells, which proliferates normally, was included as a negative control in the test. The non-proliferating minicells should not cause cell death upon the co-incubation process, even without the supplementation of antibiotics. The viability of mammalian cells was examined by LIVE/DEAD staining (invitrogen^{TM}). Green dye (calcium AM) would accumulate within only live cells. Red dye (propidium iodide) would bind to the DNA of cells (Figure 4A). Green-to-total cell ratio was calculated to measure the relative viability.

doi:10.6342/NTU202303502

The minicell-treated mammalian cells showed no significant decrease in viability at all three B/C ratios, indicates that there was no cytotoxicity by minicells. EcN mini parental cells (group Parent) caused significant (*** $p < 0.001$) decrease in cellular viability at all ratios of B/C. However, when antibiotics were included to the medium (group Parent + A), the toxicity was diminished, indicating that other bacterial components had little effect on HeLa and A549 cells.

Therefore, EcN minicells, as a non-growing portion of EcN bacterial, had minimized adverse influence on cellular viability, and with no toxicity toward HeLa and A549 cell lines.

doi:10.6342/NTU202303502

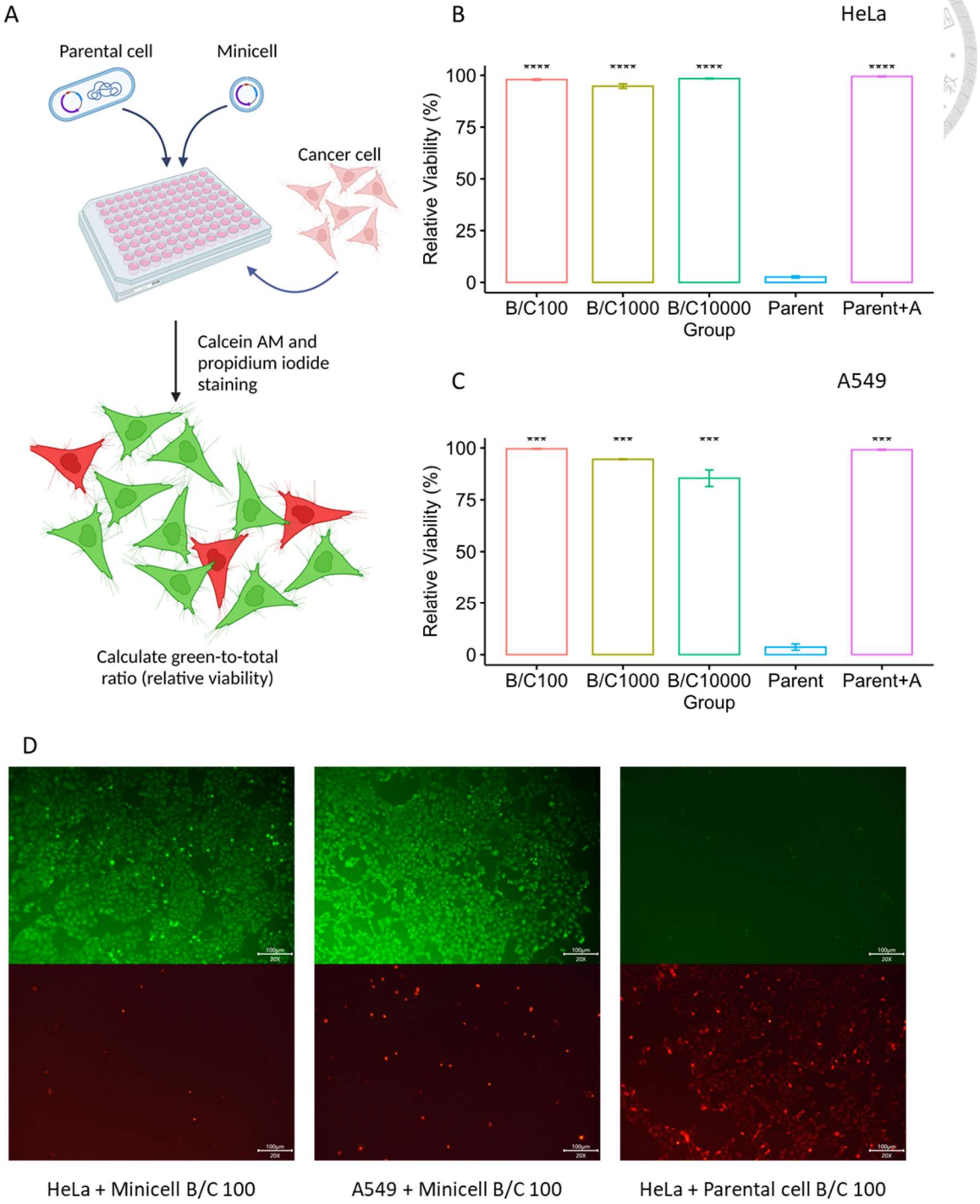

Figure 4. Cell viability test upon minicell coculture. **A)** Cell viability test was conducted while minicells/parental cells were co-incubated with HeLa/A549 cells at different B/Cs. **B)** Relative viability of HeLa. **C)** Relative viability of A549. D) Microscopy of alive

doi:10.6342/NTU202303502

(upper channel, green) and dead cell (lower channel, red) of different groups, scale bar = 100μm. ***$p < 0.001$ and **** $p < 0.0001$.

doi:10.6342/NTU202303502

3.2.2 Attachment of Minicell on Mammalian Cell by Invasin

Before delivering Cas12b RNP into target cells, whether minicells can attach to mammalian cells should first be examined. EcN mini with pT5RF was transformed with pGB2-inv-hly plasmid, which constitutively express invasin and LLO (Table 1). Invasin, as previous mentioned, could facilitate bacterial attachment to mammalian cells and subsequently trigger cellular engulfment by beta-1 integrin mediated endocytosis. HeLa cells were co-incubated with invasin-carrying minicells for 1 hour, washed, and examined under a fluorescence microscopy. Only minicell transformed with pGB2-inv-hly showed colocalization with HeLa cells. In comparison, pT5RF-only minicells (no invasin) had no significant attachment to HeLa cells (Figure 5A).

3.2.3 Engulfment of Minicells Mediated by Invasin

To further probe the dynamics of invasin-mediated adhesion and uptaking of minicells, a series of treatments were carried out. First, we co-incubated HeLa cells with minicells (pT5RF/pGB2) of B/C 2000 at 37 or 4°C for 1 hour respectively, followed by pre-warmed DPBS rinsing and 1% paraformaldehyde fixation. Next, 0.1% Triton X-100

doi:10.6342/NTU202303502

was used to permeate one set of fixed samples, while DPBS was used to treat the remaining samples. Subsequently, anti-*E. coli* antibody (Abcam^{TM}) immunofluorescence staining was then performed on all samples using a fluorescence microscope to detect the presence of extracellular or intracellular minicell epitopes. For fluorescence quantification, the effective minicell area per cell was calculated by dividing the area of fluorescence samples by the total number of cells counted in the images.

In Figure 5B, we first observed that the ratio of total stained minicells was slightly higher compared to the DPBS-treated control group when Triton X-100 was supplemented, yet no statistical difference was found. We suspected that the time span in the experiment (1 hour) was insufficient for HeLa cells to complete engulf minicells bound on the outer surfaces. The control groups kept at 4°C showed significantly lower amount of fluorescence signal as compared to the treatments at 37°C, indicating the binding might be somewhat energy- or thermal- dependent (Figure 5B).

Furthermore, we subsequently monitored the progression of minicells engulfment and intracellular dynamics in HeLa cells by using the endosomal tracking dye, Quinacrine. Using the green fluorescent dye Quinacrine, which preferentially accumulated in acidic

doi:10.6342/NTU202303502

environments (pH 5), we tracked the colocalization of red signals from minicells vs green signals from endosomes throughout the uptake process. As illustrated in Figure 5C, there was no colocalization between minicell fluorescence, red, and quinacrine signal, green, during the initial 0-1 hour co-incubation step. After 3 hours co-incubation, the red fluorescence progressively colocalized with green signal and formed yellow areas, indicating that the minicells were transported into acidic endosomes or lysosomes. After 8 hours and later (24 and 48 hours), all red fluorescence was colocalized with green fluorescence, showing us that the minicells (mCherry) were located within the acidic apparatus (e.g. lysosomes). The data showed that minicells finally were transported into the lysosomes.

doi:10.6342/NTU202303502

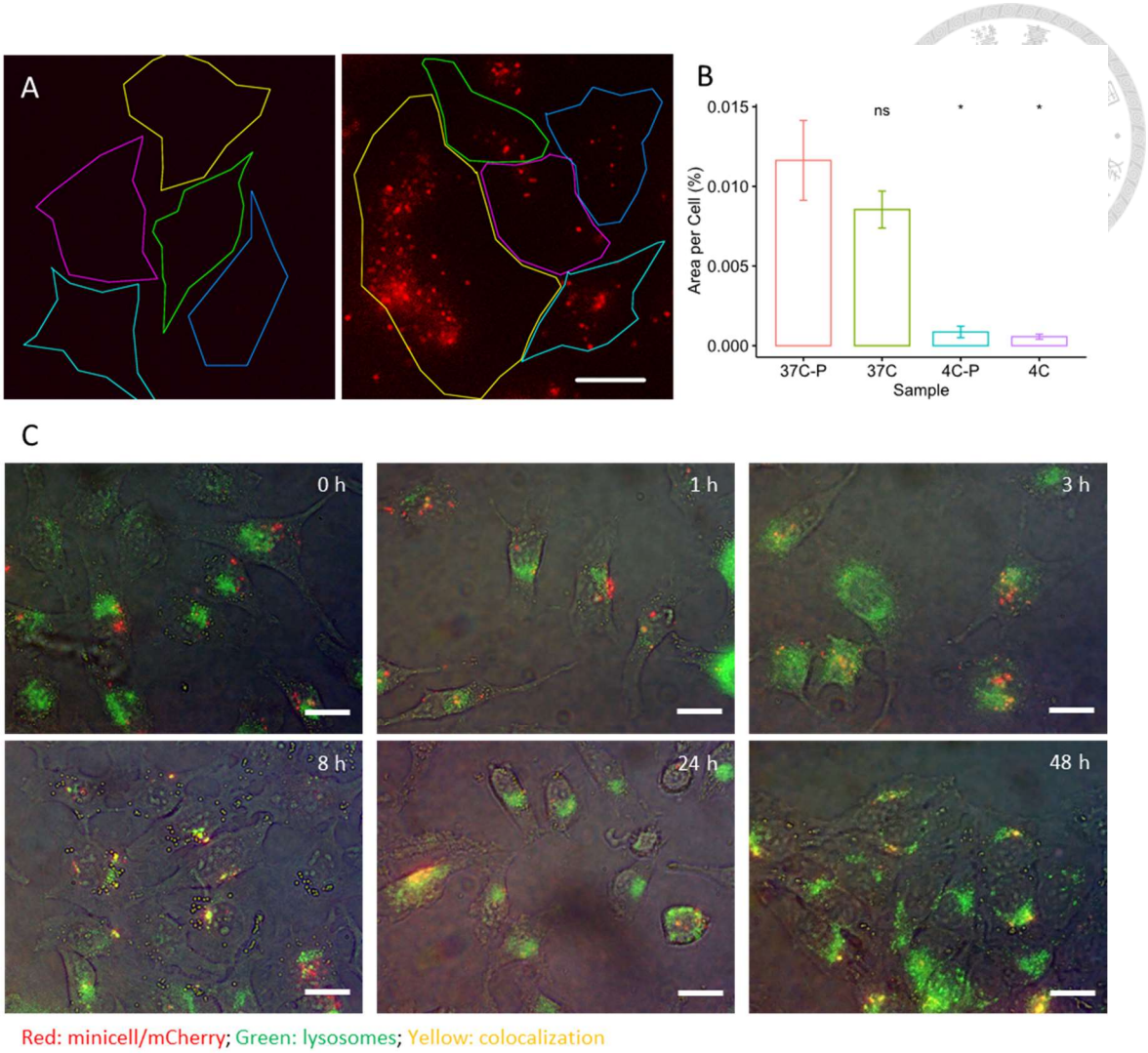

Figure 5. Binding and engulfment of *inv-hly*-expressing minicells by HeLa cells. **A)** Right channel: invasin-expressing EcN mini T5RF, red fluorescence and brightfield, with strong colocalization with HeLa cells; left channel: EcN mini T5RF without invasin, which showed no significant binding after DPBS wash. Cellular areas are separated by colored line. **B)** Minicell area per cell as determined by immunofluorescence staining. 37C-P: co-incubation at 37°C with permeabilization; 37C: co-incubation at 37°C; 4C-P: co-incubation at 4°C with permeabilization; 4C: co-incubation at 4°C. **C)** Lysosomes

doi:10.6342/NTU202303502

staining by quinacrine. Minicell colocalization (yellow) was gradually observed at time > 3 hours after co-incubation. Scale bar = 20 μm. * $p < 0.05$. ns = no significance.

doi:10.6342/NTU202303502

3.2.4 Tracking Minicell Localization within HeLa Cells

To further monitor progression and track the localization of minicell after cellular entry, another assay for minicell invasion was implemented. Specifically, HeLa cells were co-incubated with purified EcN mini pT5RF at B/C 25000 for 2 hours, rinsed with DPBS, and resupplied with fresh medium, DMEM (10% FBS) (Figure 7A). The morphology of HeLa cells and minicell fluorescence were examined along the incubation accordingly (Figure 7B). First, we have tried four different B/C ratios (100, 1000, 2000, 10000) and found that the binding is not sufficient for observation and quantification at B/C 100 (Appendix Figure 19). At B/C 1000, 2000 and 10000, the binding is sufficient for long-term observation (Figure 6A). Group B/C 10000 were observed for 96 hours after the co-incubation. Overall, the intensity of red fluorescence (mCherry/minicell) decreased day by day, but the dilution effect originated from cell division was not estimated. The majority of fluorescent signal decayed at 24-48 hours, which may imply that the minicells were transported into lysosomes before their lysis (Figure 6B).

We further tried higher B/C ratio, 25000, to figure the limitation of delivered cargo to induce cytotoxicity. 72 hours after the co-incubation, cells with higher fluorescence

doi:10.6342/NTU202303502

intensity started to die and at 96-120 hours later, only dead cells retain their fluorescence signal, indicating that this amount was somewhat toxic toward delivered cells. In previous groups (100, 1000, 2000, 10000), we did not find out any difference in viability within the samples and non-incubated negative control (data not shown).

Co-incubation at high B/C ratio, as current demonstration, could lead to efficient binding and cellular entry, but cytotoxicity could occur due to large amounts of indigestible exogenous components such as proteins, lipopolysaccharides, and endotoxins. Insufficient digestion or leakage of minicells from lysosomes may cause cellular death or apoptosis[50] in the end.

doi:10.6342/NTU202303502

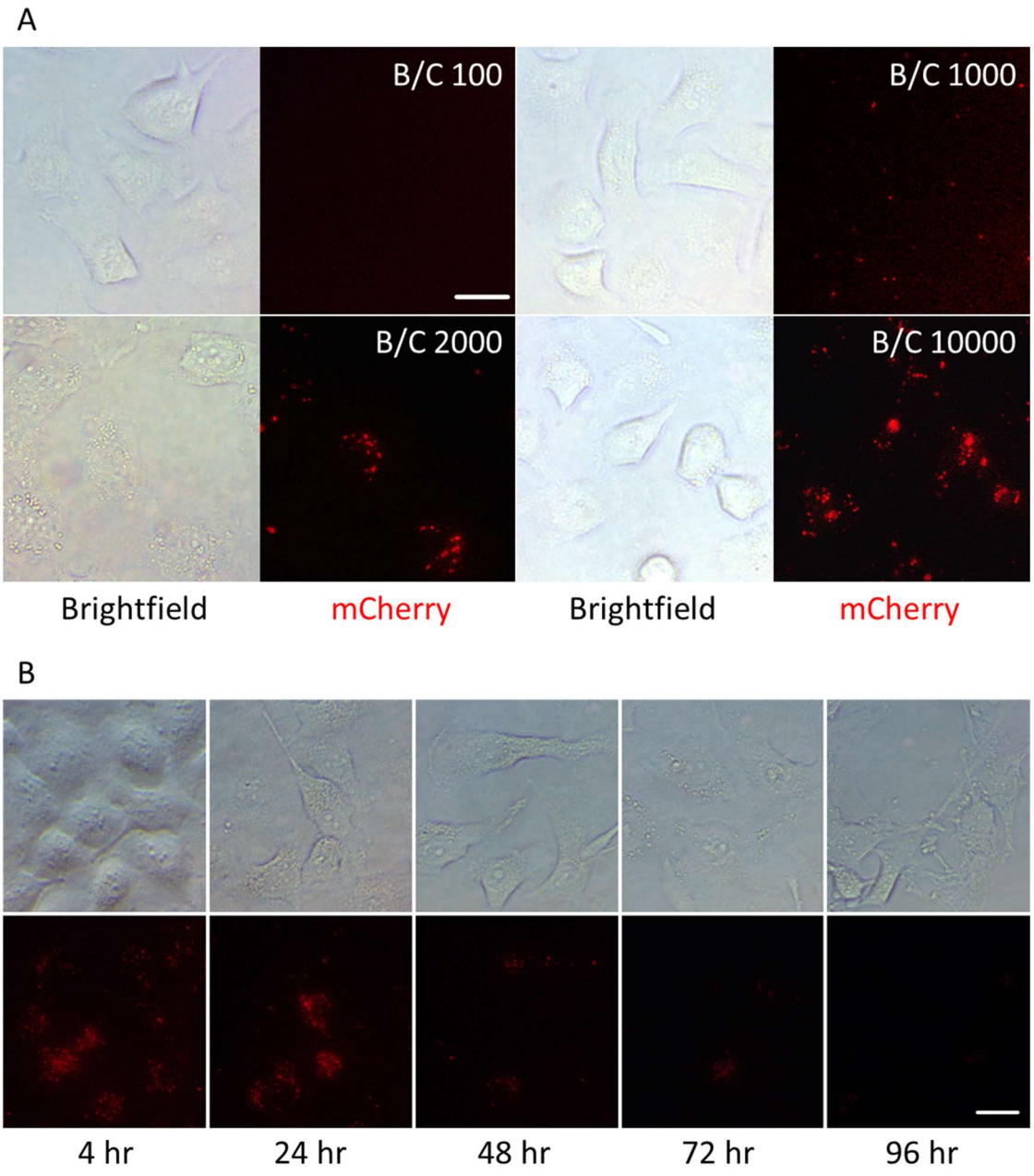

Figure 6. Minicell at different B/C ratio. **A)** Minicells and cells after co-incubation with B/C 100, 1000, 2000, 10000 at t=0 hr. **B)** At B/C 10000, cells were monitored for 96 hours after co-incubation. Scale bar = 20 μm.

doi:10.6342/NTU202303502

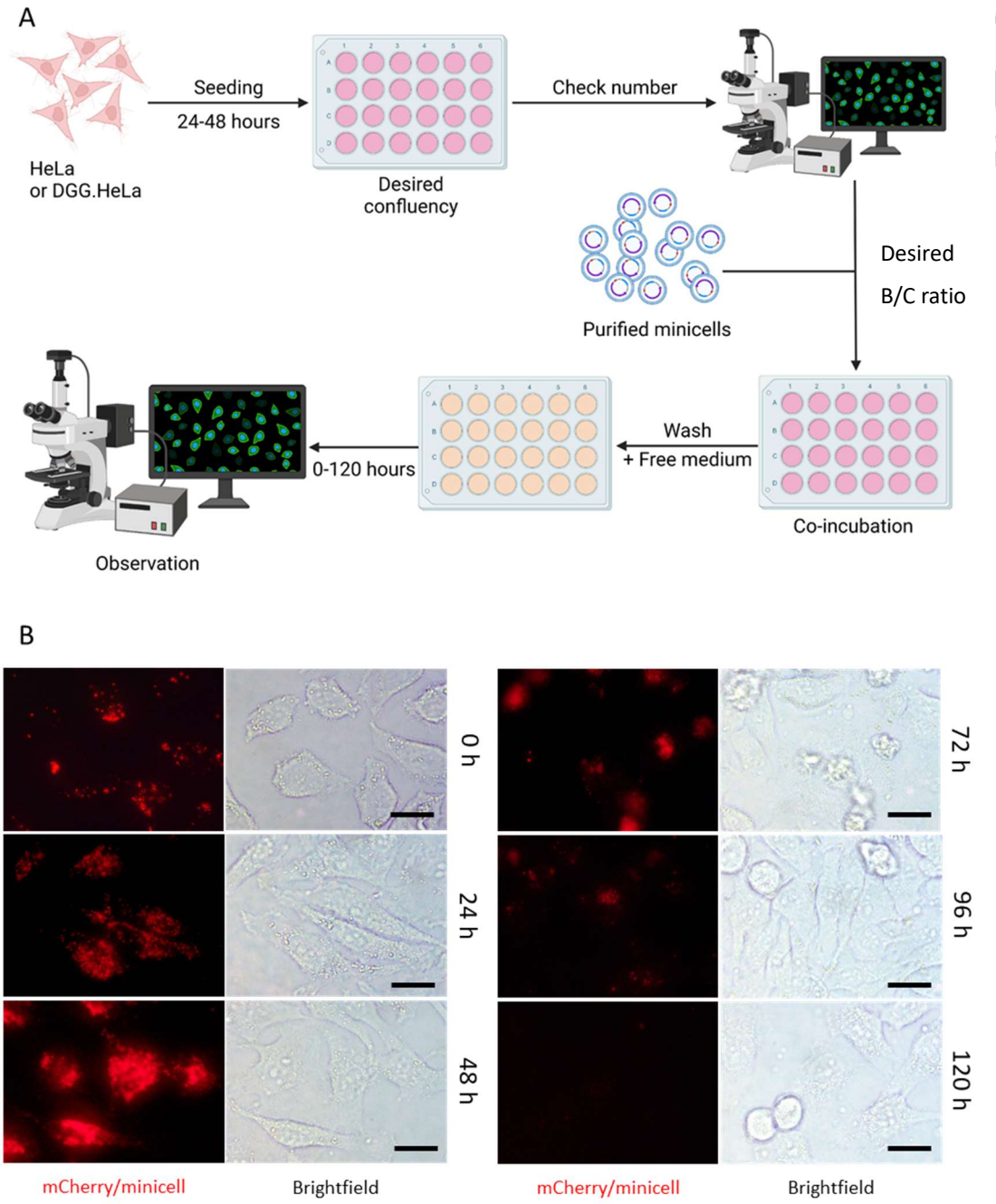

Figure 7. Minicell localization within HeLa cells. **A)** Schematic diagram of minicell delivery of mCherry into HeLa cells. **B)** mCherry/minicell localization within HeLa cells at different time point after the co-incubation. Scale bar = 20 μm.

doi:10.6342/NTU202303502

3.2.5 Lysozyme and Polymyxin B Increased Minicell Binding

In order to enhance the efficiency of cellular binding and entry of minicells, and further reduce subsequent cytotoxicity, some technical strategies are developed. In this set of experiment, we aim to increase binding at low B/C ratio, as well as to increase the release of cargos from minicells at earlier stage. To achieve so, we have utilized hen egg white lysozyme and an amphiphilic antibiotics polymyxin B to pre-treat minicells, rendering an accelerated process for minicell lysis and Cas12b RNP cargo release. Lysozyme serves to disturb bacterial cell wall by its enzymatic activity and polymyxin B acts to forms pores on bacterial outer membranes.

In the preliminary study, we examined how both chemicals affected the minicells' capacity to bind and discharge their cargo. Specifically, we incubated purified minicells with lysozyme and polymyxin B at varied concentrations, with the supplementation of 8% sucrose in 50 mM Tris-HCl buffer as for osmotic pressure protector. Under this condition, no significant lysis was found as observed (Figure 7A left) and some aggregations were found, which could be avoided by vortex and pipetting. In comparison, without the addition of 8% sucrose, some lysed minicells were observed (yellow arrow),

doi:10.6342/NTU202303502

as the intensity of fluorescence decreased and the boundaries of the minicells were disturbed (Figure 7A right). We pelleted the treated (with/without 8% sucrose) minicells, sampled the supernatant and measured its relative fluorescence reading (RFU). In Figure 7C, the group without 8% sucrose showed a significant higher reading in fluorescence, indicating the releasement of mCherry from the minicells under a hypotonic condition. The pelleted minicells w/o 8% sucrose also showed a lower intensity in fluorescence which were discernible even by naked eyes (Figure 7B).

Next, we further incubated the pretreated minicells to see the effect on cellular binding. The binding ability of invasin-expressing EcN mini in the tested conditions (lysozyme 100-1000 μg/mL, polymyxin B 10-50 μg/mL). In fact, when the concentration of both reagents was high, the binding efficiency increased (Figure 7D and 7E). Observable minicell aggregation was witnessed after lysozyme treatment by fluorescent microscope, however the effect was abolished after a gentle vertexing, and quinacrine staining showed that their engulfment was not impeded.

We were curious about whether lysozyme and polymyxin B would have synergistic effect in combination. From the heatmap illustrated in Figure 7D, the synergistic effect

doi:10.6342/NTU202303502

on binding was not observed. However, the additive effect on minicell lysis and releasement was still feasible under our primary observation.

doi:10.6342/NTU202303502

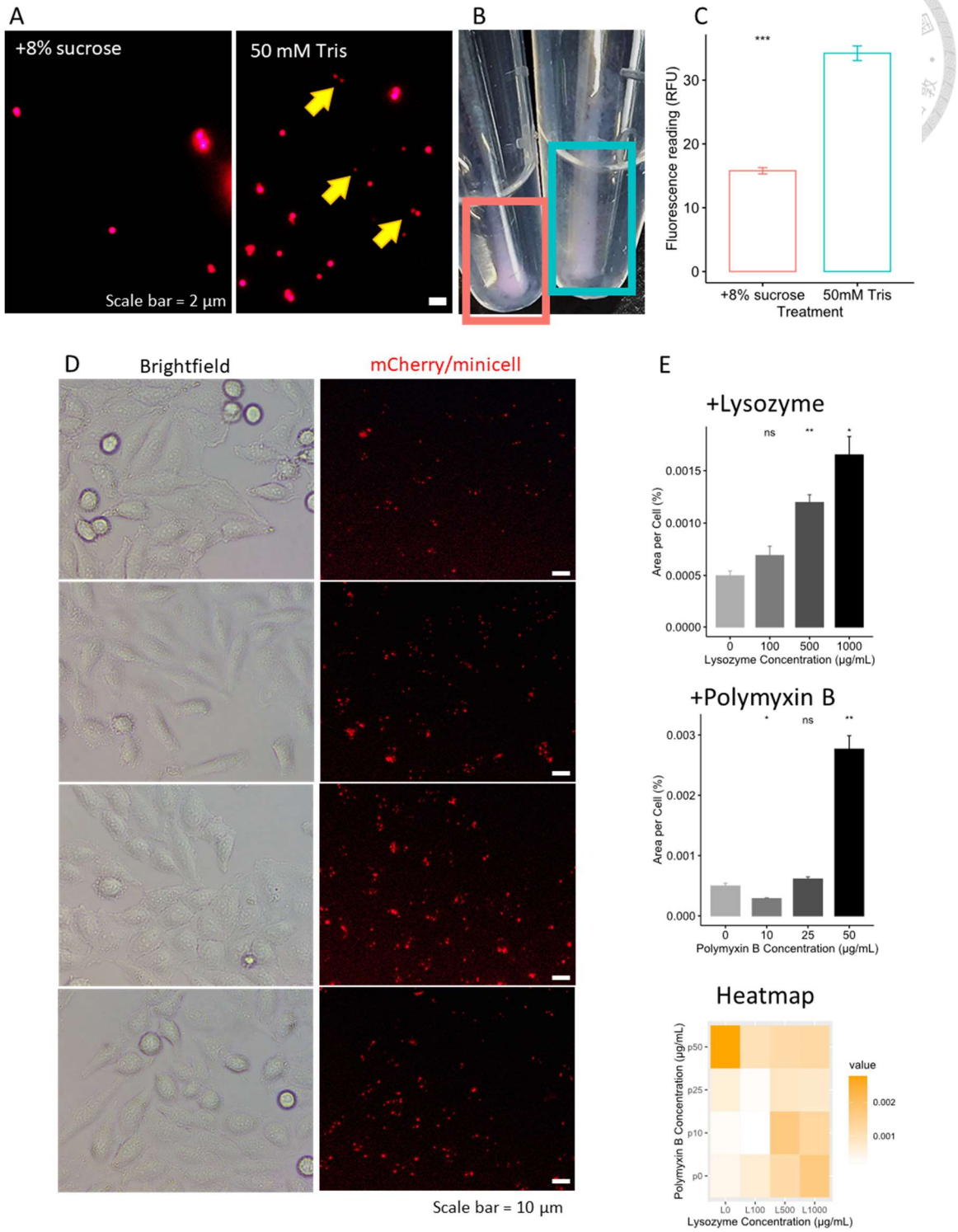

Figure 8. The effect of lysozyme and polymyxin B pretreatment on the cellular binding of minicells. **A)** The morphology of lysozyme and polymyxin B-treated minicell

doi:10.6342/NTU202303502

with/without the osmotic protection of sucrose. Yellow arrow shows partially lysed minicells with lower fluorescence intensity and compromised membranes. **B)** The pellets of protected (pink) and non-protected (blue) minicells. **C)** Measured fluorescence reading (RFU) of protected and non-protected minicells. **D)** Cellular binding of minicells after different treatment condition. N: negative control (no treatment), L0, 100, 500, 1000: lysozyme 0, 100, 500, 1000 μg/mL, P0, 10, 25, 50: polymyxin B 0, 10, 25, 50 μg/mL. **E)** Bar-plots and the heatmap of minicell binding under different treatments. *$p < 0.05$, **$p < 0.01$, ***$p < 0.001$.

3.2.6 Cargo release and migration from Lysozyme and Polymyxin B pre-treated minicells after cellular uptake

To further probe the progression of pre-treated minicells and cargo trafficking inside the cells, we tracked the migration and localization of mCherry signal from minicells in a specific region of cells over time.

From the microscopic figure (Figure 8, each color indicates one cell origin), mCherry signal from minicells distributed randomly on the HeLa cells. In later periods,

doi:10.6342/NTU202303502

mCherry signal moved into the center of HeLa cells, with observable discrimination and dispersion from 3 to 7 hours in some cells (Figure 8). The effect could come from lysosomal degradation or releasement originated from listeriolysin O. However, the majority of mCherry signal withstood until 24 hours or later, and the dispersion could be observed from 24-28 hours.

doi:10.6342/NTU202303502

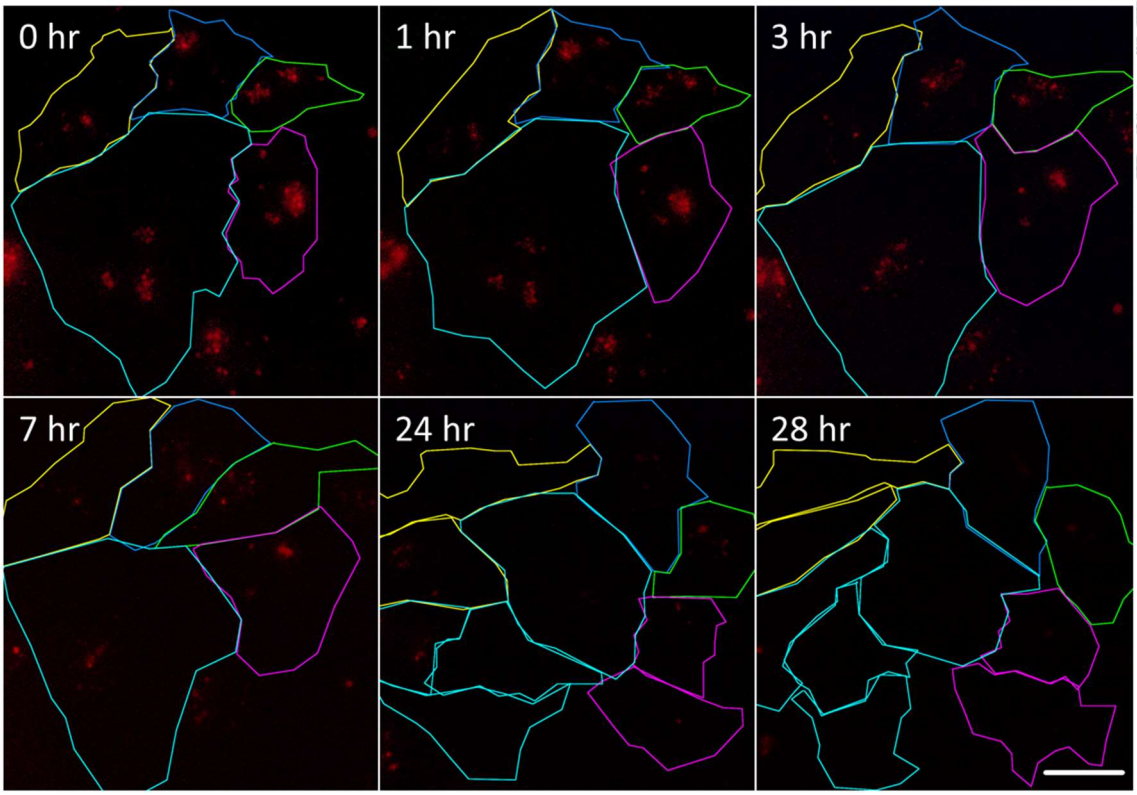

Figure 9. The distribution of mCherry signal (from pre-treated minicells) after cellular uptake within 28 hours. Each color indicates an individual cell and its daughter cells. Scale bar = 20 μm.

doi:10.6342/NTU202303502

3.3 Gene Editing

3.3.1 Establishment of DGG.HeLa Cell

Compared to loss-of-function (knockout), gain-of-function system might present a more efficient way to determine the edited cells from cell pool using fluorescence microscopy[51]. Edited cells with double strand break (DSB) in targeted site utilize either nonhomologous end join (NHEJ) or homologous direct repair (HDR) to repair the break. Error prone NHEJ usually resulted in insertion or deletion in nucleotide, causing frame-shifts in downstream gene sequence[52].

Although frameshifted genes after CRISPR editing result in truncated or even non-functional products, the remaining normal products produced prior to the DSB will take times to degrade. Exogenous proteins such as eGFP have longer half-life within host cells, which might be problematic for real time and high throughput screening. Additionally, exogenous gene expression is highly heterogenous in cancer cell lines, due to the high variation of genomic content and expression profiles in cancer cells. Those intrinsic noises, in turn, might lead to an inaccurate evaluation of gene editing solely based on the

doi:10.6342/NTU202303502

phenotypical changes by altered gene expression. In fact, we have witnessed a highly heterogenous green fluorescence distribution over time even the whole population was derived from a single mEGFP-expressing clone of cell lines. On contrary, the gain-of-function systems provides a clear-cut and more decisive outcome yet in a more responsive fashion (24-48 hours post NHEJ), and more importantly, it is not less influenced by the background noises of cancer cell lines. It might be of a better choice as a report system for CRISPR editing strategy. Here in the research, we established a DsRed-EGFP'-EGFP'' (DGG) cassette, with one in-frame *DsRed* gene, and two out-of-frame *EGFP* genes (-1 and -2) downstream of the *DsRed* gene, separated with a single-guide targeting spacer sequence and a stop codon (Figure 9B). In prior to CRISPR editing, the unaltered DGG cassette will only yield functional DsRed protein with a translational stop at the primary stop codon, which is located ahead of first GFP. After CRISPR editing against the spacer region of DGG cassette, the indel (insertion or deletion) is introduced to the spacer region by the NHEJ repairment, the primary stop codon would be disrupted, leading to fully expression of downstream (-1) or (-2) *EGFP* gene.

Subsequently, the DGG cassette was inserted into the downstream of CAG promoter in the pLAS3w.PNEO plasmid, with a neomycin resisting gene. The plasmid was

doi:10.6342/NTU202303502

prepared by PureLink™ HiPure Plasmid Midiprep Kit (Invitrogen) and transfected to A549 and HeLa cells by lipofectamine 3000 (Invitrogen) per manufacture's manual. We found that the overall transfection efficiency in A549 (Appendix Figure 16) was way lower than the efficiency for HeLa cells'. After 48 hours post transfection, 700 μg/mL of Geneticin (Gibco) was added to the medium in order to select long term expressing cells. Cells in selection were maintained under confluency by standard culturing technique. 2 weeks after Geneticin selection, positive outgrew colonies were observed in HeLa but not in A549. The positive colonies were selected using microtips and cultured in the 48-well plates with the addition of 1000 μg/mL geneticin, and eventually separated into single cell by limiting dilution (Figure 9A). Monoclones were outgrew and stored in liquid nitrogen.

doi:10.6342/NTU202303502

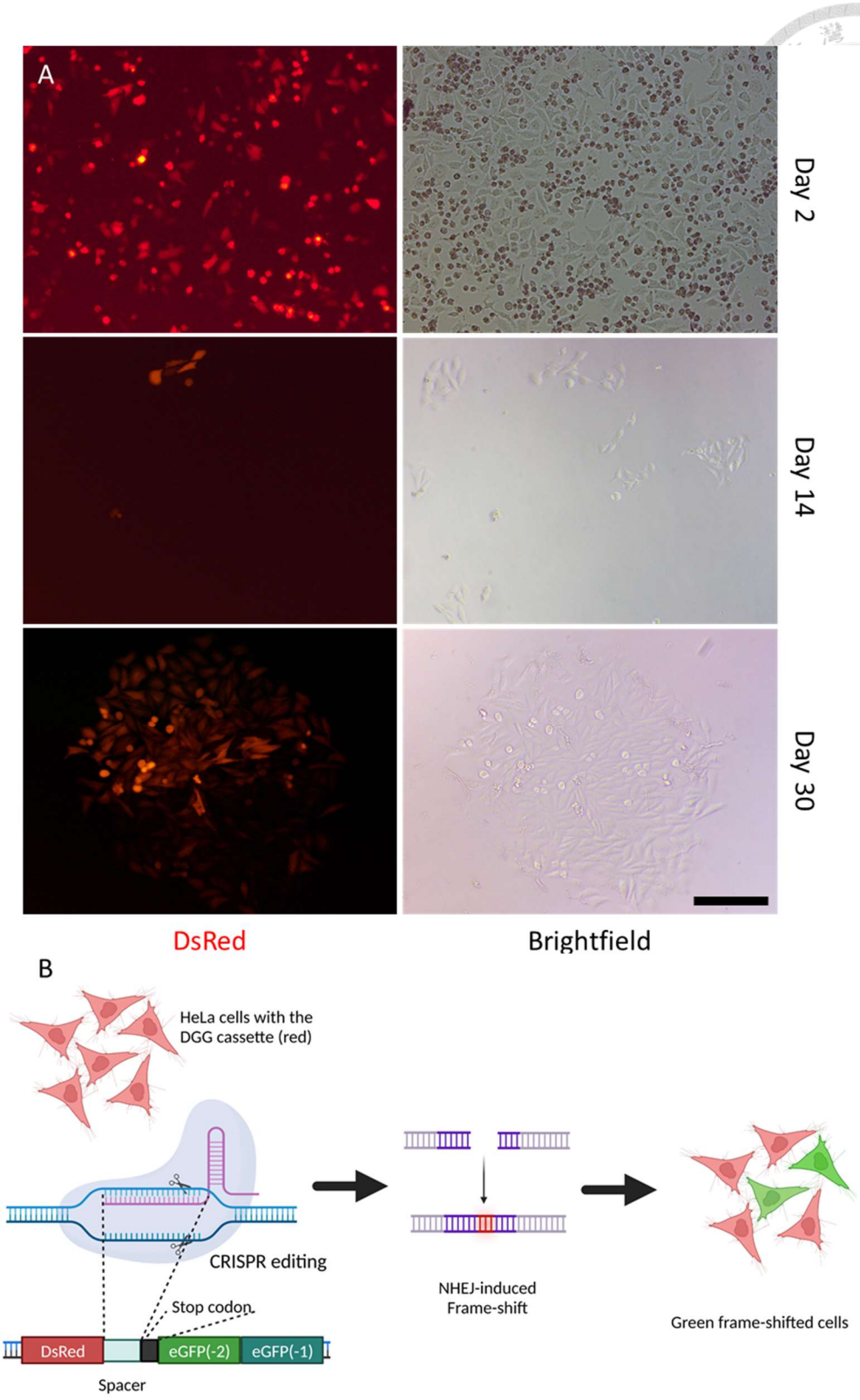

Figure 10. Establishment of DGG.HeLa cell line. **A)** HeLa cells at day 2, day 14, and day 30 post-transfection. The antibiotic selection started at day 2. The DsRed expressing

doi:10.6342/NTU202303502

stable cell population at day 14 and the outgrowth of single clone at day 30. Scale bar = 100 μm. **B)** The schematic graph of gain-of-function DGG reporter.

3.3.2 Cas12b RNP Cleavage in Electroporated DGG.HeLa Cell

We first need to test whether the DGG cell line can correctly report the edited phenotype under a positive treatment. Cas12b RNP with sgSpacer sequence was induced and purified from an EcN mini culture baring the pACYC-Cas12b-sgSpacer sequence. Purified Cas12b RNP was diluted into 1 mg/mL in 50 mM Tris-HCl buffer (pH 8.0) and stored at 4°C for no more than 2 days.

For the validation of DGG.HeLa cell clones, we tried direct delivery of Cas12b RNP via lipofection (Lipofectamine 3000) and electroporation (BTX ECM 630, exponential wave). As the results indicated in Figure 10A, lipofection by Lipofectamine 3000 showed a lower efficiency regardless of the amount than that of electroporation. When performing electroporation, a variety of parameters was evaluated for optimal efficiency. It was found that the ideal condition was set at 1000V/cm, 200 μF, no resistance. At the higher energy over 1000V/cm, 200 μF for delivery (e.g. higher voltage per length, higher current, higher

doi:10.6342/NTU202303502

resistance), the lower the viability of the cells was observed, rendering no overall enhancement in the editing efficiency.

In Figure 10B, the electroporated cells had a death ratio of ~50% (1000 V/cm, 200 μF, no resistance), with no difference between the control, BSA, or sample, Cas12b RNP. Negative control (BSA-transfected or no electrical pulse) showed completely no green cells in the end by the examination under the fluorescence microscopy. Green-to-red ratio (green cell number/red cell number) varied from 2.5-6.8%, at the concentration range of 5-30 μg Cas12b RNP/10^6 cells. There was no significant difference among sample treatments (5, 10, 20, 30 μg of Cas12b RNP), yet the samples were all significant higher in editing efficiency (**$p < 0.01$), in comparison to negative controls (BSA, NC).

doi:10.6342/NTU202303502

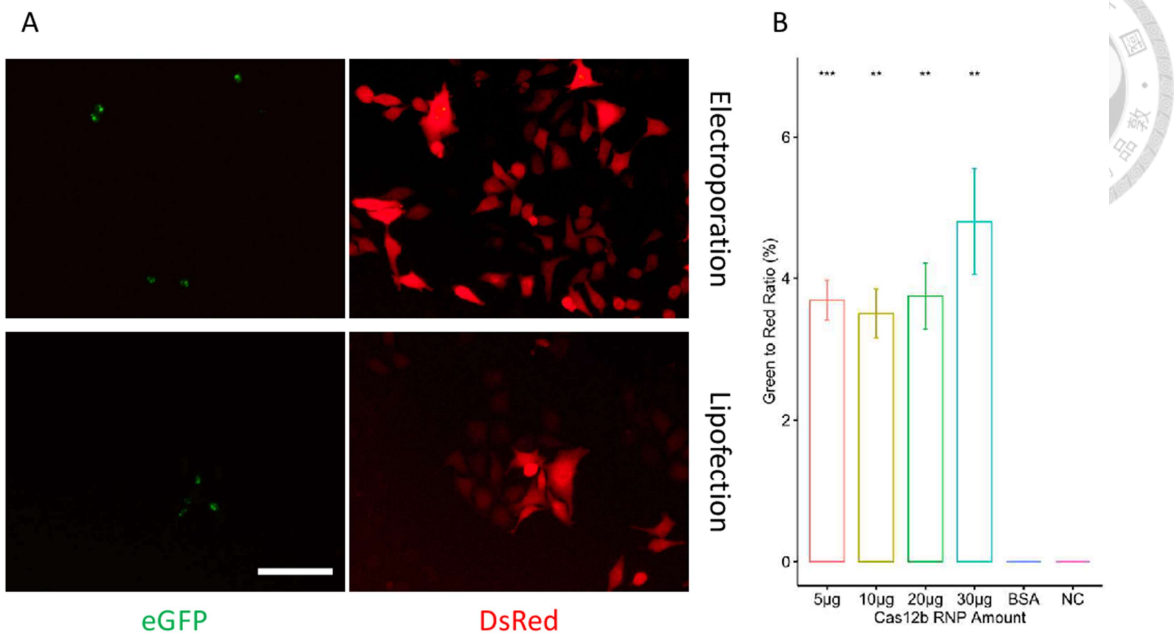

Figure 11. Cas12b RNP delivery for DGG.HeLa editing by electroporation and lipofection. **A)** Positive (green) cells in all (red) cells were shown in both (electroporation and lipofection) group. Scale bar = 100 μm. **B)** Green-to-red ratio of delivered cells with different delivered amount (5-30 μg) and the controls (BSA and NC no electrical pulse). **p < 0.01, ***p < 0.001.

3.3.3 Cas12b RNP Delivery by Lysozyme and Polymyxin B-Treated Minicell

Finally, we aimed to evaluate the efficiency of CRISPR editing mediated by the modified minicell delivery approach. Minicells carrying Cas12b:sgSpacer (sample) and Cas12b:sgEGFP (control) with invasin and listeriolysin O were purified, followed by co-

doi:10.6342/NTU202303502

incubation with DGG.HeLa cells at a B/C ratio of 2000:1 (10^5 cells in individual 24-wells) for 1 hour, in which the minicells were pretreated with lysozyme (500 μg/mL), polymyxin B (50 μg/mL), or together. For comparison, un-pretreated minicells carrying the same cargos above were also used in the test, serving as the control groups. After sterile DPBS rinsing and fresh medium (10% FBS in DMEM with 500 μg/mL G418) supplementation, each treatment was monitoring over 24-72 hours. Cells were subsequently passaged when reaching confluency.

As the results depicted in Figure 11, there were green cells (edited cells) observed in groups L500, P50, L500P50 under the sgSpacer treatment groups at 48 hours post co-incubation. The ratio of green cells in each treatment remained consistent over time. P50 had a highest edited ratio of 4.4 ± 0.6 %, then L500P50 (2.7 ± 0.7 %) and L500 (1.9 ± 0.2 %). There were no green cells observed in negative controls sgEGFP (NC) and untreated (UT) minicells. This, in turn, provided a solid evidence showing the great promise of using minicells for CRISPR delivery and cell editing. Yet the fabrication processes and editing efficiency of the minicells are to be further optimized in the future.

doi:10.6342/NTU202303502

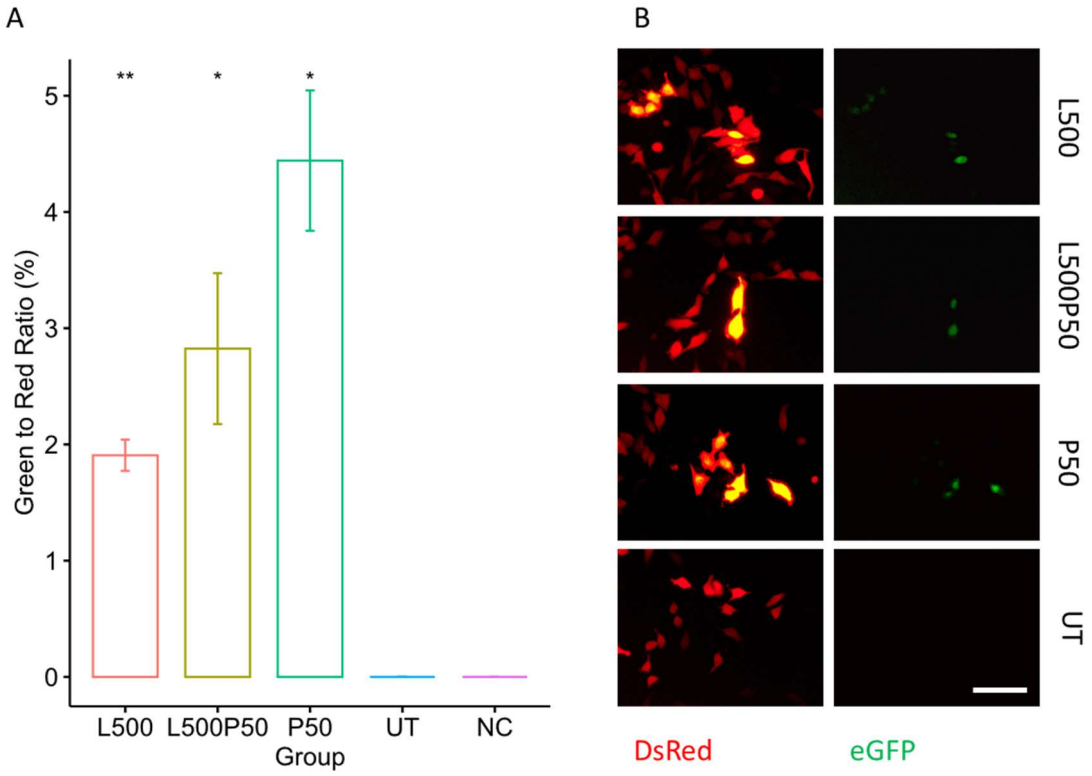

Figure 12. Cas12b RNP Delivery and DGG.HeLa cell editing by pretreated minicells. **A)** Green-to-red ratio in different groups, significance was compared toward group NC (UT: untreated, NC: negative control (sgEGFP)). **B)** Phenotype of edited cells in each group. Scale bar = 100 μm. *p < 0.05, **p < 0.01.

doi:10.6342/NTU202303502

4. Conclusion and Discussion

In conclusion, we have demonstrated that:

1. Successful generation of minicell phenotype by *minCD* knockout in EcN strain.

2. Separation and purification of minicells from a parental-minicell mixing population.

3. Recombinant protein production (mCherry and Cas12b) in EcN mini strain and the accumulate of recombinant proteins in minicells.

4. Cas12b RNP purified from minicell portion remain active in a in vitro dsDNA cleavage test.

5. Pure minicells were test no acute toxicity toward cancer cell line HeLa and A549.

6. Invasin-expressing minicells were capable of cellular binding and entry.

7. Minicells, after the engulfment, final localized in acidic apertures such as lysosomes, by lysosomal staining.

8. The addition of lysozyme and polymyxin B can largely enhance the binding efficiency of minicells toward mammalian cells.

Minicell, beside its ability to accumulate recombinant proteins after expression as its parental cell does, show some interesting features. First, when the recombinant protein

doi:10.6342/NTU202303502

forms inclusion bodies, which usually distribute at two poles of the parental cells, minicell tend to contain a higher ratio of the recombinant protein in comparison to parental cells[53]. This may due to the asymmetric division start site, in which the majority of the inclusion body is “removed” into the minicell, as minicell originates from the pole of the parental cells. Second, we found that *minCD* knockout strain has a higher expression content of recombinant Cas12b protein compared to normal EcN wildtype. As confirmed by SDS-PAGE and CBR staining, both purified minicells and mixture from EcN mini strain showed deeper band of Cas12b than EcN wildtype showed, when the same amount of cell weight was used. These features indicate that *minCD*-knockout EcN or other *E. coli* strain may have advantage in producing inclusion body-forming recombinant proteins. Other researchers also found that the deficiency in *minCD* may lead to changes in cellular metabolism, resulting in higher tolerance toward antibiotics and increased $NADH/NAD^+$ ratio[54]. They demonstrated that this feature can increase toxic chemical production yield.

Minicells are usually chromosome-free. As a delivery platform, it is an advantage to minimize the influence of the vector. Although minicells contain the same protein composition and surface lipopolysaccharide as their parental cells, the lack of

doi:10.6342/NTU202303502

chromosomal DNA can largely eliminate the contamination from bacterial chromosomal DNA. When facing plasmid or gene delivery, the utilization of minicell will be superior toward whole bacterial cell delivery system.

Lysosomal staining by quinacrine results indicate that minicells require about >3 hours to finally transferred into acidic apertures. From the pKa of quinacrine, we have a rough calculation that quinacrine accumulate in the environment where the pH < 5, indicating the precise staining of lysosomes. All minicells containing vacuoles mature to lysosome within 24 hours. However, as observed under the fluorescence microscope, the majority of minicell and its fluorescence remains intact even until 48 hours, showing the insufficient degradation by lysosomes in HeLa cells.

The reason why polymyxin B and lysozyme can increase cellular binding remain unclear. Lysozyme, in higher concentration, stimulates aggregation only when bacterial cells (parental/minicell) exist. This may origin from the anchoring effect of lysozyme into bacteria outer membrane. Under isotonic buffer environment, no significant lysis was observed, indicating that the aggregation is not from cytosolic component such as proteins or DNAs. The aggregation can be abolished by strong vortex, and the majority of

doi:10.6342/NTU202303502

minicells stay homogenously distribution within the co-incubation process. Polymyxin B, in comparison, causes no aggregation under the concentration below 1 mg/mL. We hypothesize that after lysozyme or polymyxin B treatment, minicells' surface charge was altered, resulting in higher opportunity to be in contact with mammalian cell surface. Normal bacterial cells are negatively charged as same as mammalian cells. Therefore, with the alternation of surface charge minicells could be more easily attracted to mammalian cells by electrostatic interactions. Both lysozyme and polymyxin B are positively charged, if the major barrier between bacteria and mammalian cell is their charges, it is not surprise that the addition of lysozyme and polymyxin B can enhance minicell binding.

Treatment of polymyxin B and lysozyme can significantly decreased the viability of parental cells culture[55-57]. These can be originated from their pore-forming and wall-degrading activity. Parental cells losing its structural integrity will be susceptible to outer environment such as osmotic pressure, resulting in cell death and lysis. In minicell model, however, lysozyme and polymyxin B cannot lead to significant lysis within an isotonic buffer environment. Minicells withstand the destruction from polymyxin B and lysozyme, probably because they cannot further proliferate or grow in size, preventing them from

doi:10.6342/NTU202303502

intrinsic enlargement of volume, which finally lead to lysis. After be engulfed into endosome, weakly acidic late endosome (pH~5.5) could not allow effective lysis of minicell. If the lysis is postponed to the maturation of lysosome (pH~4.5), minicell component such as Cas12b RNP and listeriolysin O would be susceptible to degradative enzymes, causing insufficient delivery. Moreover, a research has indicated that the optimal working environment of listeriolysin O is as intermediate to late endosome (pH = 5.5-6), and lysosomal pH is too low for effective membrane disruption. From our observation, optimal lysosomal degradation of minicells was exhibited at 24-48 hours post minicell invasion in HeLa cells. However, even after 72 hours, intact minicells could still be found within live cells, indicating insufficient degradation by lysosomes. If particles within lysosomes are undegradable, cells could exclude them by exocytosis. Minicells components are either degraded within lysosome because of ineffective listeriolysin O, or excluded due to insufficient degradation.

AaCas12b, as reported, has a similar activity as SpCas9 *in vivo* and *in vitro*, with a lower off-target rate in long-term exposure (i.e. by plasmid transfection)[16]. Similar to Cas9, AaCas12b activity is largely affected by its targeting sequence, or gRNA complementary sequence. As showed in the *in vitro* cleavage test, sgSpacer had a lower

doi:10.6342/NTU202303502

cleavage ratio compared to sgEGFP when the same amount of dsDNA was added, indicating that the spacer sequence is not optimal for double-strand break. Lower off-target rate may be explained as lower activity *in vivo*, and when the concentration is below the threshold of action, Cas12b might have a lower activity toward target sequence as compared to Cas9.

doi:10.6342/NTU202303502

5. Future Work and Perspective

Minicells have superior advantages, such as chromosomal DNA-free, high protein loading, low toxicity, high stability, and small size. However, in our delivery system, its stability becomes a large barrier for efficient cargo releasement. Normal methods promoting bacterial lysis such as auxotrophy and antibiotics treatment are limited in the minicell delivery models. As we hypothesize, we should advance the lysis before lysosomal maturation (i.e. when minicells are still reside in endosome) for successful escape and cargo delivery. There are several ways to promote lysis before lysosomal maturation: first, expressing phage lysis protein such as holin, endolysin, and spanin, which are essential to lytic phage as their terminal releasement from bacterial cells [58]. Holin mediates the permeabilization of bacterial inner membrane, endolysin degrades bacterial cell wall, and spanin trigger the fusion of inner and outer membrane[59]. In an isotonic environment, both three components are required for sufficient lysis of host cell. There has been already research utilizing lambda phage lysis gene to trigger bacterial lysis upon invasion, resulting in cargo releasement within the cell. Second, the addition of lysosomotropic agents or ATPase-inhibitors can postpone the maturation of lysosomes, which allows the lysis occur within late endosomes. Third, by expressing short

doi:10.6342/NTU202303502

membrane-insertion peptide that only active at low pH, the membrane structure can be affected at endosomal environment, allowing efficient releasement only at pH < 6.

Polymyxin B and lysozyme show a promising enhancement for cellular binding in this research. In the future study, the effects of both reagents on cellular delivery will be further evaluated Additionally, EcN auxotrophic strain EcN *dapA*-, with the deficiency in cell wall synthesis, established from our lab, will be investigated as a new and potential EcN model for cargo delivery We anticipate to build up an innovative and yet efficient vehicle for future therapeutics delivery with elevated cost-effectiveness and safety using the probiotic minicell systems.

doi:10.6342/NTU202303502

6. Reference

1. Scheller, E.L. and P.H. Krebsbach, *Gene therapy: design and prospects for craniofacial regeneration.* J Dent Res, 2009. **88**(7): p. 585-96.
2. Gonçalves, G.A.R. and R.M.A. Paiva, *Gene therapy: advances, challenges and perspectives.* Einstein (Sao Paulo), 2017. **15**(3): p. 369-375.
3. Arabi, F., V. Mansouri, and N. Ahmadbeigi, *Gene therapy clinical trials, where do we go? An overview.* Biomedicine & Pharmacotherapy, 2022. **153**: p. 113324.
4. Westermann, L., B. Neubauer, and M. Köttgen, *Nobel Prize 2020 in Chemistry honors CRISPR: a tool for rewriting the code of life.* Pflugers Arch, 2021. **473**(1): p. 1-2.
5. Urnov, F.D., et al., *Genome editing with engineered zinc finger nucleases.* Nature Reviews Genetics, 2010. **11**(9): p. 636-646.
6. Ghosh, D., A. Kumar, and N. Sinha, *Chapter 6 - Targeted genome editing: a new era in molecular biology*, in *Advances in Animal Genomics*, S. Mondal and R.L. Singh, Editors. 2021, Academic Press. p. 75-89.

doi:10.6342/NTU202303502

7. Gaj, T., C.A. Gersbach, and C.F. Barbas, *ZFN, TALEN, and CRISPR/Cas-based methods for genome engineering.* Trends in Biotechnology, 2013. **31**(7): p. 397-405.

8. Ishino, Y., et al., *Nucleotide sequence of the iap gene, responsible for alkaline phosphatase isozyme conversion in Escherichia coli, and identification of the gene product.* J Bacteriol, 1987. **169**(12): p. 5429-33.

9. Gostimskaya, I., *CRISPR–Cas9: A History of Its Discovery and Ethical Considerations of Its Use in Genome Editing.* Biochemistry (Moscow), 2022. **87**(8): p. 777-788.

10. Cong, L., et al., *Multiplex genome engineering using CRISPR/Cas systems.* Science, 2013. **339**(6121): p. 819-23.

11. Mali, P., et al., *RNA-guided human genome engineering via Cas9.* Science, 2013. **339**(6121): p. 823-6.

12. Ebrahimi, V. and A. Hashemi, *Challenges of in vitro genome editing with CRISPR/Cas9 and possible solutions: A review.* Gene, 2020. **753**: p. 144813.

13. Anders, C., et al., *Structural basis of PAM-dependent target DNA recognition by the Cas9 endonuclease.* Nature, 2014. **513**(7519): p. 569-73.

doi:10.6342/NTU202303502

14. Shmakov, S., et al., *Discovery and Functional Characterization of Diverse Class 2 CRISPR-Cas Systems.* Molecular Cell, 2015. **60**(3): p. 385-397.

15. Gurel, F., et al., *On- and Off-Target Analyses of CRISPR-Cas12b Genome Editing Systems in Rice.* Crispr j, 2022.

16. Teng, F., et al., *Repurposing CRISPR-Cas12b for mammalian genome engineering.* Cell Discovery, 2018. **4**(1): p. 63.

17. Uddin, F., C.M. Rudin, and T. Sen, *CRISPR Gene Therapy: Applications, Limitations, and Implications for the Future.* Frontiers in Oncology, 2020. **10**.

18. Wang, H.-X., et al., *CRISPR/Cas9-Based Genome Editing for Disease Modeling and Therapy: Challenges and Opportunities for Nonviral Delivery.* Chemical Reviews, 2017. **117**(15): p. 9874-9906.

19. Duan, L., et al., *Nanoparticle Delivery of CRISPR/Cas9 for Genome Editing.* Frontiers in Genetics, 2021. **12**.

20. Yip, B.H., *Recent Advances in CRISPR/Cas9 Delivery Strategies.* Biomolecules, 2020. **10**(6).

21. Crudele, J.M. and J.S. Chamberlain, *Cas9 immunity creates challenges for CRISPR gene editing therapies.* Nature Communications, 2018. **9**(1): p. 3497.

doi:10.6342/NTU202303502

22. Weiss, S. and T. Chakraborty, *Transfer of eukaryotic expression plasmids to mammalian host cells by bacterial carriers.* Current Opinion in Biotechnology, 2001. **12**(5): p. 467-472.

23. Darji, A., et al., *Oral Somatic Transgene Vaccination Using Attenuated S. typhimurium.* Cell, 1997. **91**(6): p. 765-775.

24. Dietrich, G., et al., *Delivery of antigen-encoding plasmid DNA into the cytosol of macrophages by attenuated suicide Listeria monocytogenes.* Nature Biotechnology, 1998. **16**(2): p. 181-185.

25. Grillot-Courvalin, C., et al., *Functional gene transfer from intracellular bacteria to mammalian cells.* Nature Biotechnology, 1998. **16**(9): p. 862-866.

26. Duong, M.T.-Q., et al., *Bacteria-cancer interactions: bacteria-based cancer therapy.* Experimental & Molecular Medicine, 2019. **51**(12): p. 1-15.

27. Muralinath, M., et al., *Immunization with Salmonella enterica serovar Typhimurium-derived outer membrane vesicles delivering the pneumococcal protein PspA confers protection against challenge with Streptococcus pneumoniae.* Infect Immun, 2011. **79**(2): p. 887-94.

doi:10.6342/NTU202303502

28. Lin, I.Y., T.T. Van, and P.M. Smooker, *Live-Attenuated Bacterial Vectors: Tools for Vaccine and Therapeutic Agent Delivery.* Vaccines (Basel), 2015. **3**(4): p. 940-72.

29. Chen, Q., et al., *Induction of Protein Expression Within Escherichia coli Vector for Entry into Mammalian Cells.* Human Gene Therapy Methods, 2013. **25**(1): p. 40-47.

30. Chung, T.-C., et al., *Improved Escherichia coli Bactofection and Cytotoxicity by Heterologous Expression of Bacteriophage ΦX174 Lysis Gene E.* Molecular Pharmaceutics, 2015. **12**(5): p. 1691-1700.

31. Akinsola, R.O., et al., *Inhibition of lysosomal vacuolar proton pump down-regulates cellular acidification and enhances E. coli bactofection efficiency.* Analytical Biochemistry, 2021. **616**: p. 114088.

32. Zhang, Y., et al., *E. coli Nissle 1917-Derived Minicells for Targeted Delivery of Chemotherapeutic Drug to Hypoxic Regions for Cancer Therapy.* Theranostics, 2018. **8**(6): p. 1690-1705.

33. Giacalone, M.J., et al., *The use of bacterial minicells to transfer plasmid DNA to eukaryotic cells.* Cellular Microbiology, 2006. **8**(10): p. 1624-1633.

doi:10.6342/NTU202303502

34. Sonnenborn, U., *Escherichia coli strain Nissle 1917—from bench to bedside and back: history of a special Escherichia coli strain with probiotic properties.* FEMS Microbiology Letters, 2016. **363**(19): p. fnw212.

35. Lynch, J.P., L. Goers, and C.F. Lesser, *Emerging strategies for engineering Escherichia coli Nissle 1917-based therapeutics.* Trends in Pharmacological Sciences, 2022. **43**(9): p. 772-786.

36. Li, R., et al., *Expressing cytotoxic compounds in Escherichia coli Nissle 1917 for tumor-targeting therapy.* Research in Microbiology, 2019. **170**(2): p. 74-79.

37. Zhang, Y., et al., *Escherichia coli Nissle 1917 Targets and Restrains Mouse B16 Melanoma and 4T1 Breast Tumors through Expression of Azurin Protein.* Applied and Environmental Microbiology, 2012. **78**(21): p. 7603-7610.

38. Lehouritis, P., et al., *Activation of multiple chemotherapeutic prodrugs by the natural enzymolome of tumour-localised probiotic bacteria.* Journal of Controlled Release, 2016. **222**: p. 9-17.

39. Bai, F., et al., *Bacterial type III secretion system as a protein delivery tool for a broad range of biomedical applications.* Biotechnol Adv, 2018. **36**(2): p. 482-493.

40. Adler, H.I., et al., *MINIATURE escherichia coli CELLS DEFICIENT IN DNA*.* Proceedings of the National Academy of Sciences, 1967. **57**(2): p. 321-326.

doi:10.6342/NTU202303502

41. Farley, M.M., et al., *Minicells, Back in Fashion.* J Bacteriol, 2016. **198**(8): p. 1186-95.

42. Yu, X., et al., *Bioengineered Escherichia coli Nissle 1917 for tumour-targeting therapy.* Microbial Biotechnology, 2020. **13**(3): p. 629-636.

43. Jivrajani, M. and M. Nivsarkar, *Ligand-targeted bacterial minicells: Futuristic nano-sized drug delivery system for the efficient and cost effective delivery of shRNA to cancer cells.* Nanomedicine: Nanotechnology, Biology and Medicine, 2016. **12**(8): p. 2485-2498.

44. MacDiarmid, J.A., et al., *Sequential treatment of drug-resistant tumors with targeted minicells containing siRNA or a cytotoxic drug.* Nature Biotechnology, 2009. **27**(7): p. 643-651.

45. MacDiarmid, J.A., et al., *Bacterially Derived 400 nm Particles for Encapsulation and Cancer Cell Targeting of Chemotherapeutics.* Cancer Cell, 2007. **11**(5): p. 431-445.

46. Sonnenborn, U. and J. Schulze, *The non-pathogenic Escherichia coli strain Nissle 1917 – features of a versatile probiotic.* Microbial Ecology in Health and Disease, 2009. **21**(3-4): p. 122-158.

doi:10.6342/NTU202303502

47. Jivrajani, M., N. Shrivastava, and M. Nivsarkar, *A combination approach for rapid and high yielding purification of bacterial minicells.* Journal of Microbiological Methods, 2013. **92**(3): p. 340-343.

48. Datsenko, K.A. and B.L. Wanner, *One-step inactivation of chromosomal genes in Escherichia coli K-12 using PCR products.* Proceedings of the National Academy of Sciences, 2000. **97**(12): p. 6640-6645.

49. Bornhorst, J.A. and J.J. Falke, *Purification of proteins using polyhistidine affinity tags.* Methods Enzymol, 2000. **326**: p. 245-54.

50. Wang, F., R. Gómez-Sintes, and P. Boya, *Lysosomal membrane permeabilization and cell death.* Traffic, 2018. **19**(12): p. 918-931.

51. de Jong, O.G., et al., *A CRISPR-Cas9-based reporter system for single-cell detection of extracellular vesicle-mediated functional transfer of RNA.* Nature Communications, 2020. **11**(1): p. 1113.

52. Xue, C. and E.C. Greene, *DNA Repair Pathway Choices in CRISPR-Cas9-Mediated Genome Editing.* Trends Genet, 2021. **37**(7): p. 639-656.

53. Kim, S.-J., W. Chang, and M.-K. Oh, *Escherichia coli minicells with targeted enzymes as bioreactors for producing toxic compounds.* Metabolic Engineering, 2022. **73**: p. 214-224.

doi:10.6342/NTU202303502

54. Kim, S.-J. and M.-K. Oh, *Minicell-forming Escherichia coli mutant with increased chemical production capacity and tolerance to toxic compounds.* Bioresource Technology, 2023. **371**: p. 128586.

55. Derde, M., et al., *Hen Egg White Lysozyme Permeabilizes Escherichia coli Outer and Inner Membranes.* Journal of Agricultural and Food Chemistry, 2013. **61**(41): p. 9922-9929.

56. Jones, C.H., et al., *Polymyxin B Treatment Improves Bactofection Efficacy and Reduces Cytotoxicity.* Molecular Pharmaceutics, 2013. **10**(11): p. 4301-4308.

57. Zhu, C., et al., *Conjugated Polymer-Coated Bacteria for Multimodal Intracellular and Extracellular Anticancer Activity.* Advanced Materials, 2013. **25**(8): p. 1203-1208.

58. Young, R., *Phage lysis: three steps, three choices, one outcome.* J Microbiol, 2014. **52**(3): p. 243-58.

59. Cahill, J. and R. Young, *Chapter Two - Phage Lysis: Multiple Genes for Multiple Barriers*, in *Advances in Virus Research*, M. Kielian, T.C. Mettenleiter, and M.J. Roossinck, Editors. 2019, Academic Press. p. 33-70.

doi:10.6342/NTU202303502

7. Appendix

7.1 Primers and sgRNA Used in the Research

Table 3. Primers used in this research.

Name	Sequence
PF-T5RBS-6xHis	TTAAAGAGGAGAAATTAACCATGCATCATCATCATCATCATCTCG
PR-mCherry-T7T	GCCGGATCGTTGAGCTCTTACTTGTACAGCTCGTCCATGC
PF-mC(C')-T7T	TAAGAGCTCAACGATCCGGCTGCTAACAAAGCCCGAAAGG
PR-pACYC2-RBS	GGTTAATTTCTCCTCTTTAATGAATTCTGTG
PF-DsRed-NheI	atataGCTAGCATGGATAGCACTGAGAACGTCATC

doi:10.6342/NTU202303502

PR-SV40pA-EcoRI	TCTCGAGGTCGAGAATTCTAAGATACATTGATGAGTTTGGACAAACCAC
sgEGFP	gtctaaaggacagaatttttcaacgggtgtgccaatggccact ttccaggtggcaaagcccgttgaacttcaagcgaagtggcac (Scaffold) tggctgttgtagt (Targeted sequence)
sgSpacer	gtctaaaggacagaatttttcaacgggtgtgccaatggccact ttccaggtggcaaagcccgttgaacttcaagcgaagtggcac (Scaffold) tttccctcccagtcccttggctat (Targeted sequence)

doi:10.6342/NTU202303502

7.2 Plasmid Map

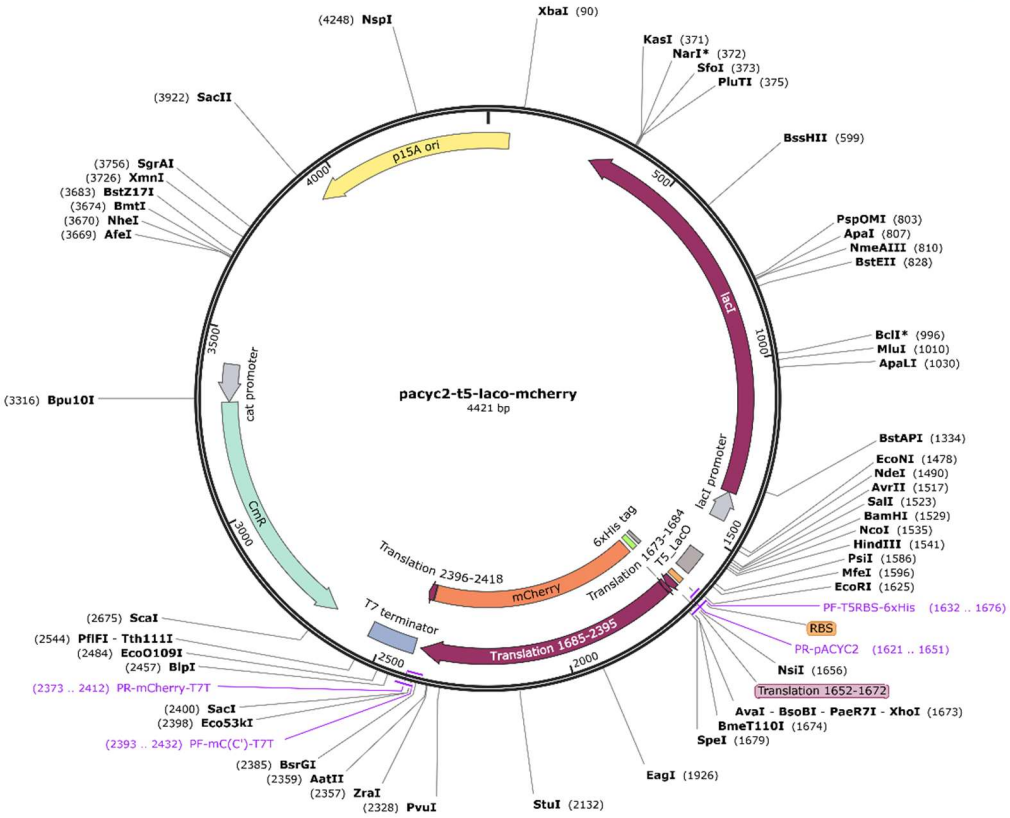

Figure 13. pACYC2-T5lacO-mCherry

doi:10.6342/NTU202303502

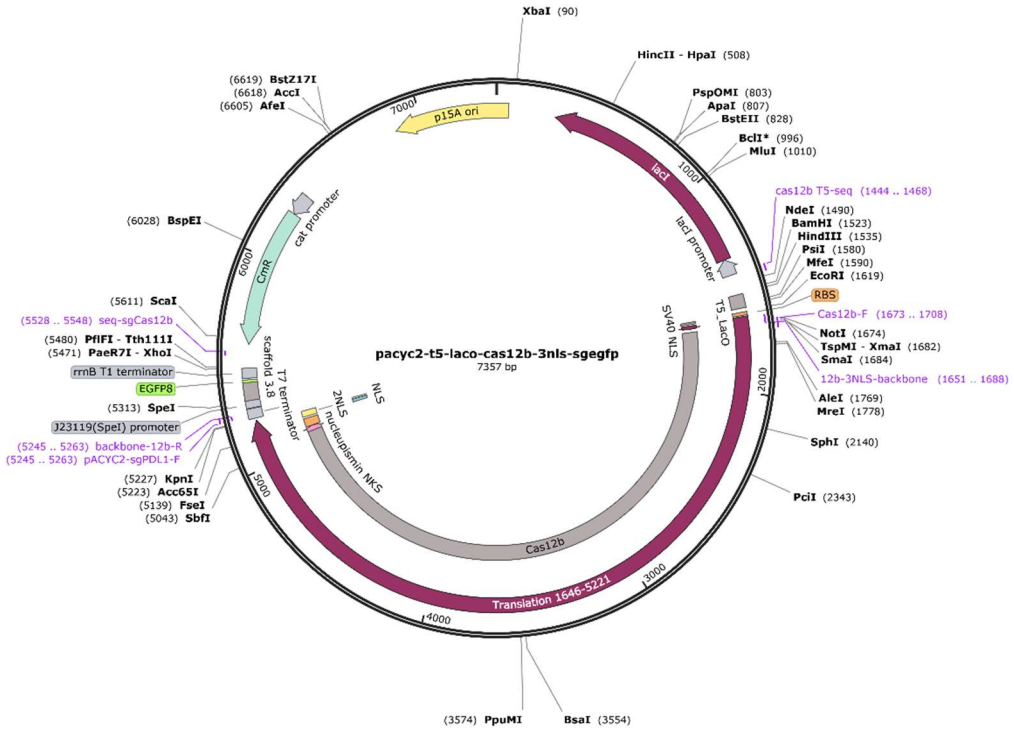

Figure 14. pACYC2-T5lacO-Cas12b-3NLS-sgEGFP

doi:10.6342/NTU202303502

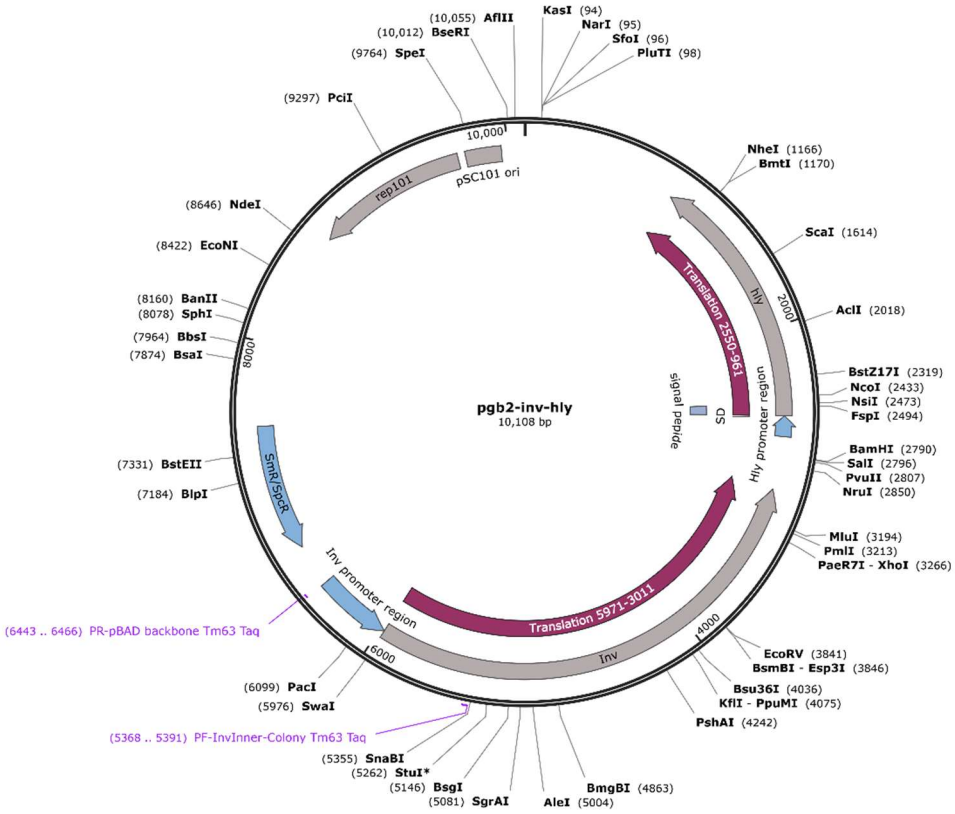

Figure 15. pGB2-inv-hly

doi:10.6342/NTU202303502

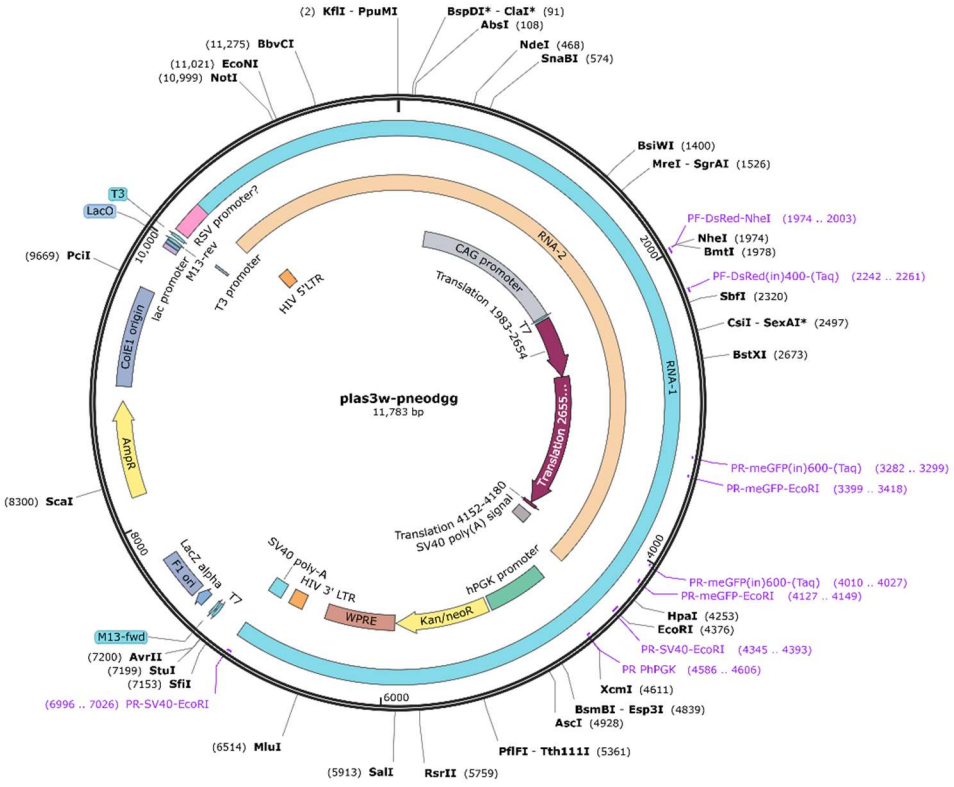

Figure 16. pLAS3w-PNEO(DGG)

doi:10.6342/NTU202303502

7.3 G418 Sensitivity Test

Table 4. G418 sensitivity of HEK293, A549, and HeLa cells

G418	ug/mL	0	50	100	200	300	400	500	600	700	800	900	1000
HEK293	D0	0	0	0	0	0	0	0	0	0	0	0	0
	D2	0	0	0	0	0	0	0	1	1	1	1	1
	D4	0	0	0	0	0	1	2	2	2	3	3	3
	D5	0	0	0	0	0	1	2	2	3	3	4	4
	D6	0	0	0	0	0	1	2	3	4	4	4	4
	D7(end)	0	0	0	0	0	1	3	4	4	4	4	4
A549	D0	0	0	0	0	0	0	0	0	0	0	0	0
	D2	0	0	0	0	0	0	0	0	0	0	0	0
	D4	0	0	0	0	0	0	0	0	1	1	2	2
	D5	0	0	0	0	0	0	1	1	2	3	3	3
	D6	0	0	0	0	0	1	2	3	3	4	4	4
	D7(end)	0	0	0	0	1	2	3	3	3	4	4	4
Hela	D0	0	0	0	0	0	0	0	0	0	0	0	0
	D2	0	0	0	0	0	0	0	1	1	1	1	1
	D4	0	0	0	0	0	1	1	2	3	3	4	4
	D5	0	0	0	0	1	1	2	3	4	4	4	4
	D6(end)	1	1	1	1	2	3	4	4	4	4	4	4

The degree of death (0-4) was determined manually by WST-1 assay (TaKaRa™); 0: 100% of cells are alive; 1: <25% of cells are dead; 2: <50% of cells are dead; 3: <75% cells are dead; 4: <100% cells are dead.

doi:10.6342/NTU202303502

7.4 Transfection of DGG to A549

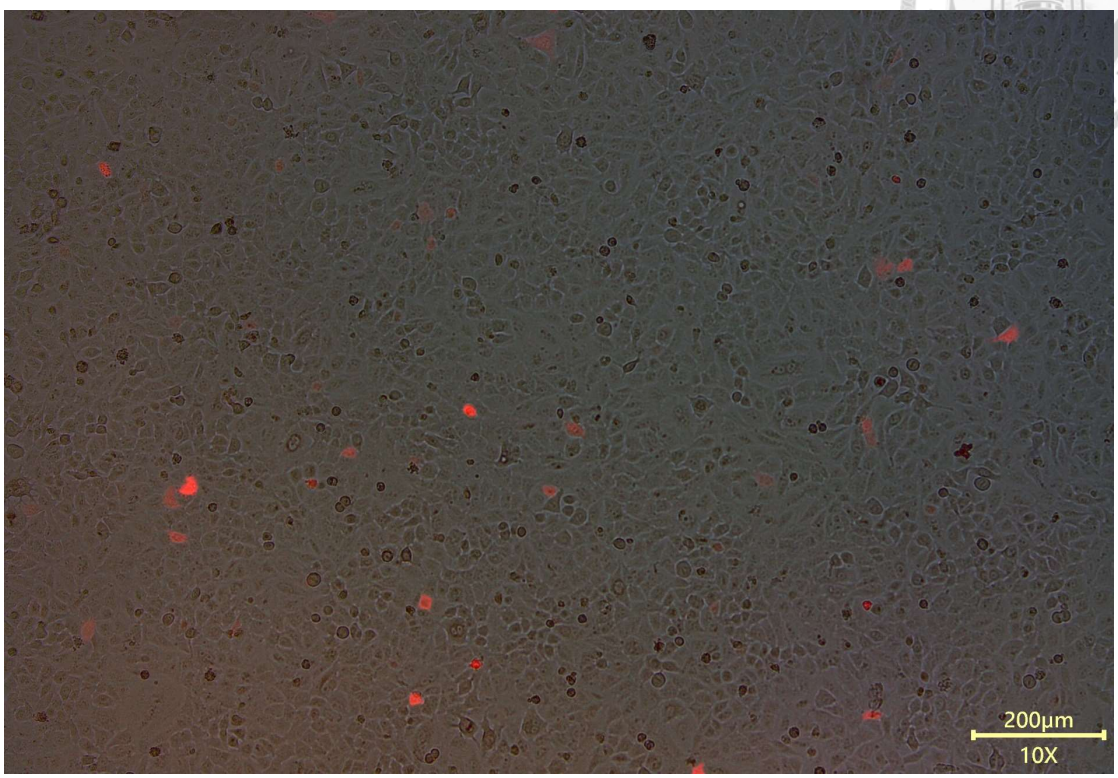

Figure 17. Merged image of transfected A549, 2 days after the transfection was conducted. The transfected red A549 cells failed to proliferate. Scale bar = 200 μm.

doi:10.6342/NTU202303502

7.5 Immunofluorescence Staining

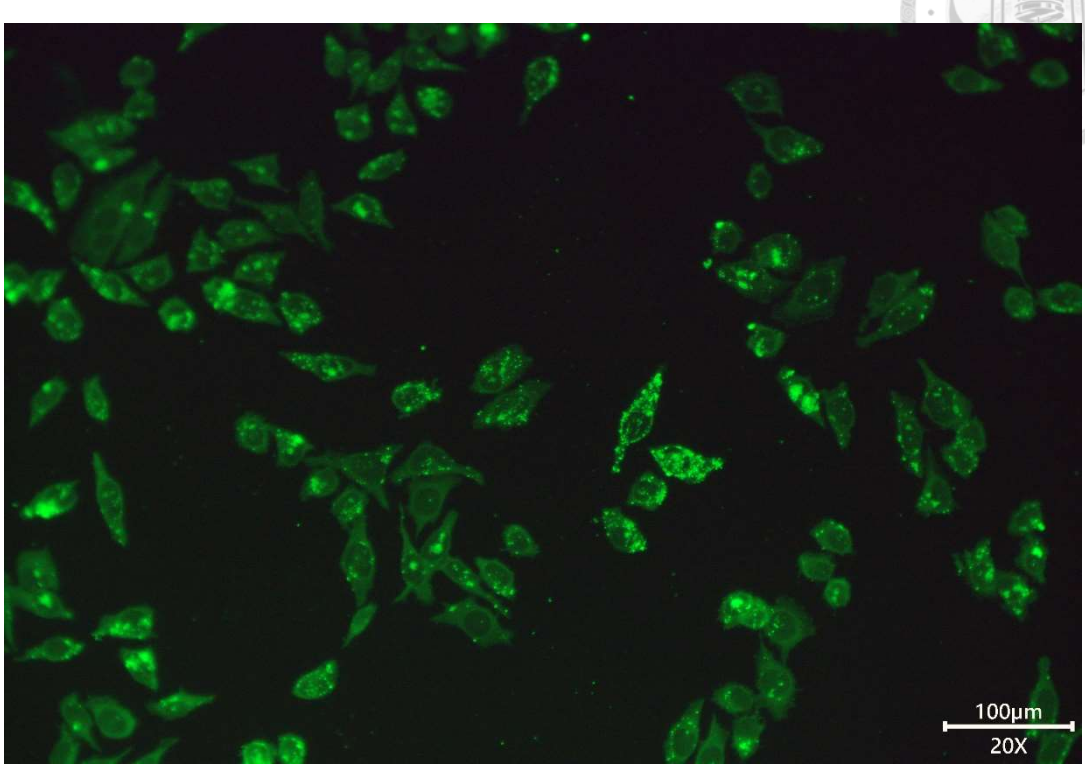

Figure 18. HeLa cells co-incubated with EcN mini 12Sp/GB2 at 37°C for 2 hours. Scale bar = 100 μm.

doi:10.6342/NTU202303502

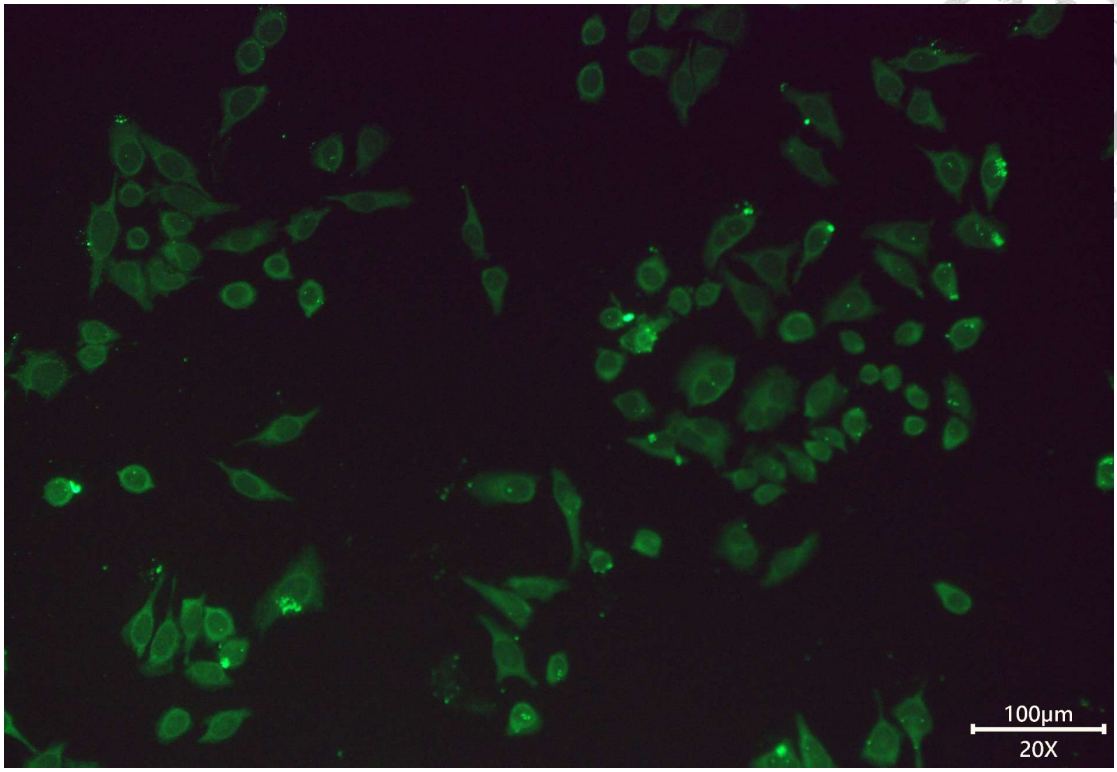

Figure 19. HeLa cells co-incubated with EcN mini 12Sp/GB2 at 4°C for 2 hours. Scale bar = 100 μm.

doi:10.6342/NTU202303502

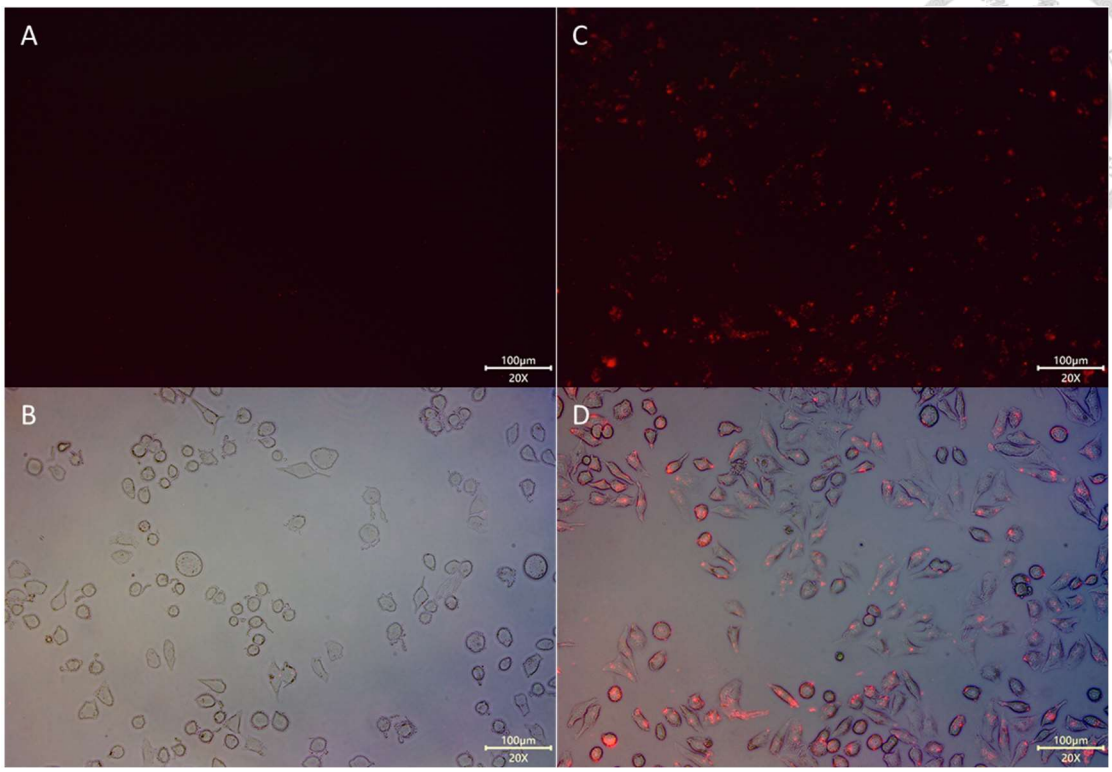

Figure 20. Minicell attachment at B/C 100 and 2000. **A)** mCherry (red fluorescence) channel at B/C 100. **B)** Merged image of brightfield and mCherry channel at B/C 100. **C)** mCherry (red fluorescence) channel at B/C 2000. **D)** Merged image of brightfield and mCherry channel at B/C 2000. Scale bar = 100 μm.

doi:10.6342/NTU202303502

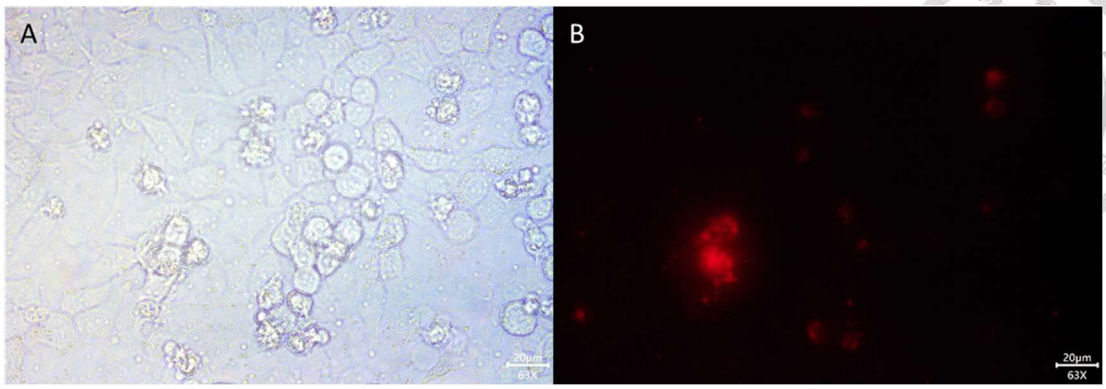

Figure 21. 144 hours post incubation. **A)** Brightfield and **B)** mCherry channel at 144 hours post minicells co-incubation with HeLa cells.

doi:10.6342/NTU202303502